LATE CRETACEOUS (CAMPANIAN AND MAASTRICHTIAN) SEQUENCE STRATIGRAPHY, SOUTHEASTERN NORTH CAROLINA, USA

Jessica A. Pierson

A Thesis Submitted to the
University of North Carolina at Wilmington in Partial Fulfillment
Of the Requirements for the Degree of
Master of Science

Department of Earth Sciences

University of North Carolina at Wilmington

2003

Approved by

Advisory Committee

_____ _____

_____
Chair

Accepted by

_____
Dean, Graduate School

This thesis has been prepared in the style and format

Consistent with the journal

Southeastern Geology

TABLE OF CONTENTS

ABSTRACT

Sequence stratigraphic analysis using samples, geophysical logs, and biostratigraphic data from U.S.G.S. core holes Kure Beach, Hilton Park, and Black Rock Landing identified four partial or complete Late Cretaceous sequences. Sequence 1 (Campanian) is dominated by dirty calcareous sand. Mean sand size is 1.93 φ; mean carbonate wt. % is 25.9%. This partial sequence is interpreted as a highstand systems tract (HST). A Type-1 sequence boundary separates Sequence 1 from the next sequence; it is reflected by an irregular surface and the absence of calcareous nannofossil zones CC24 and CC25a. Sequence 2 (Maastrichtian) is characterized in its lower part by clean, fining-upward (1.7 φ to 3.4 φ) calcareous sand interpreted as a lowstand wedge (LSW). The LSW is overlain by a grainstone followed by calcareous sand with a mean sand size of 2.92 φ and a mean wt. % carbonate of 65.2%, interpreted as a transgressive systems tract (TST). The overlying HST is dominated by intercalated muddy carbonate, skeletal grainstone, and mollusk-fragment carbonate sand. Mean sand size is 2 φ; mean wt. % carbonate is 39.3%. A Type-2 sequence boundary separates Sequence 2 from the next sequence. Sequence 3 consists of a basal coarsening-upwards calcareous sand that is interpreted as a shelf margin deposit (SMST). Mean sand size is 2.63 φ; mean wt. % carbonate is 34.1%. A sharp contact separates the SMST from the overlying TST. Mean grain size fines to 3.12φ and mean wt. % carbonate increases to 47.4%. The condensed interval (CI) occurs where sediment size is the finest; no hardgrounds are present. The overlying HST consists of a lower parasequence that shoals upward from muddy to sandy carbonate with evidence of storm winnowing. Mean grain size is 2.64 φ; mean wt. % carbonate is 51.8%. The younger parasequence shoals to a sandy, pelecypod-mold grainstone. Mean sand size is 1.64 φ; mean wt % carbonate is 56.7 %. A dissolution surface above the grainstone represents the 68 Ma unconformity. The youngest

sequence (4) has variable lithology. The Cretaceous parts consist of a nearly pure carbonate overlain by muddy sand. Mean sand size is 2.61 φ; mean weight % carbonate is 26.9

ACKNOWLEDGMENTS

I would like to thank the Department of Earth Sciences at the University of North Carolina for both their monetary and academic support. I would also like to thank the Northeastern New Hanover Conservancy for providing funding for my project.

Thanks also go to Jean Self-Trail of the U.S. Geological Survey for providing me with biostratigraphic correlations for sections of the Kure Beach core. This data enabled me to support my findings and was greatly appreciated. I would also like to thank Kathleen Farrell and Bill Hoffman of the North Carolina Geological Survey for their assistance with core sampling.

Special thanks go to my thesis committee members, Dr. Patricia Kelley and Dr. Paul Thayer, for giving me their ideas and feedback. I would especially like to thank my committee chair, Dr. Bill Harris, for being an outstanding advisor and mentor.

I would like to also thank the following people who have helped me along the way: Dr. Lynn Leonard, Dr. Sue Kezios, Roger Shew, Karen Shafer and SMEC, Cathy Morris, Tammy Auger, C.J. Jackson, Beth Reimer, Ben McGinnis, Alisha Renfro, Kenneth Willson, John Welsh, Jeff Marshall, my brother, John, and my very considerate boyfriend, Adam.

Last, but not least, I would like to thank my parents, Kim and Mary Margaret, who have always been my greatest champions and whose love and support mean more than I could ever express.

LIST OF TABLES

LIST OF FIGURES

INTRODUCTION

Cretaceous exposures of the North Carolina Coastal Plain have been studied and discussed since Stephenson (1912) first described them along the Cape Fear River. Subsequent workers (Heron, 1958; Swift, 1964; Heron and Wheeler, 1964; Sohl and Owens 1991) have sought to refine his interpretation; however, much of the stratigraphy of the area remains problematic. These problems are due, in part, to the lack of distinctly mappable surfaces, lithologic similarities within and between units, and limited exposures. Previous studies of these stratigraphic units have been based on lithology and paleontologic characteristics. No attempt has been made, however, to apply sequence stratigrapic concepts to units in the Cape Fear River area. The purpose of this project is to study the Upper Cretaceous Donoho Creek and Peedee Formations in three cores recently completed by the U. S. Geological Survey between Black Rock Landing on the Cape Fear River, Hilton Park on the Northeast Cape Fear River, and Kure Beach, N.C. (Fig. 1). These cores form a 35-mile dip line from updip Black Rock Landing to downdip Kure Beach. Through core analysis, sequences, sequence boundaries and associated systems tracts are tied to previously described outcrops of the Donoho Creek and Peedee Formations exposed in the Cape Fear River valley (Figs. 2a and b). This approach enables the construction of a three-dimensional sequence stratigraphic framework for Upper Cretaceous (Campanian and Maastrichtian) units in the Cape Fear Arch area of the southeastern Atlantic Coastal Plain.

Historical Background

Stephenson (1912, 1923) first described the stratigraphy of the Upper Cretaceous in North and South Carolina. His work created a base for many other workers seeking to provide a stratigraphic framework for Cretaceous units in North Carolina; however, due to a scarcity of

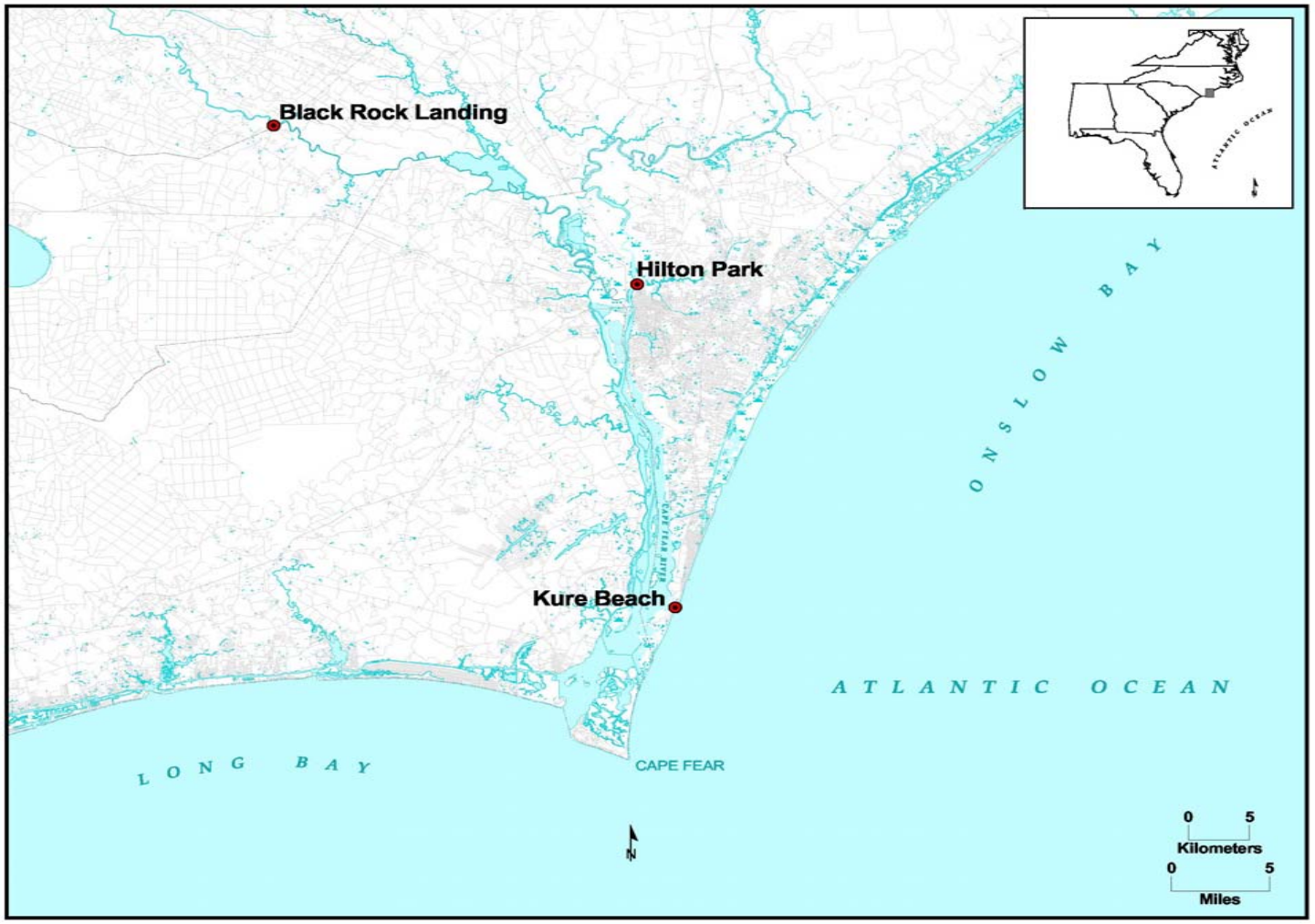

Figure 1. Location map of study area showing core holes.

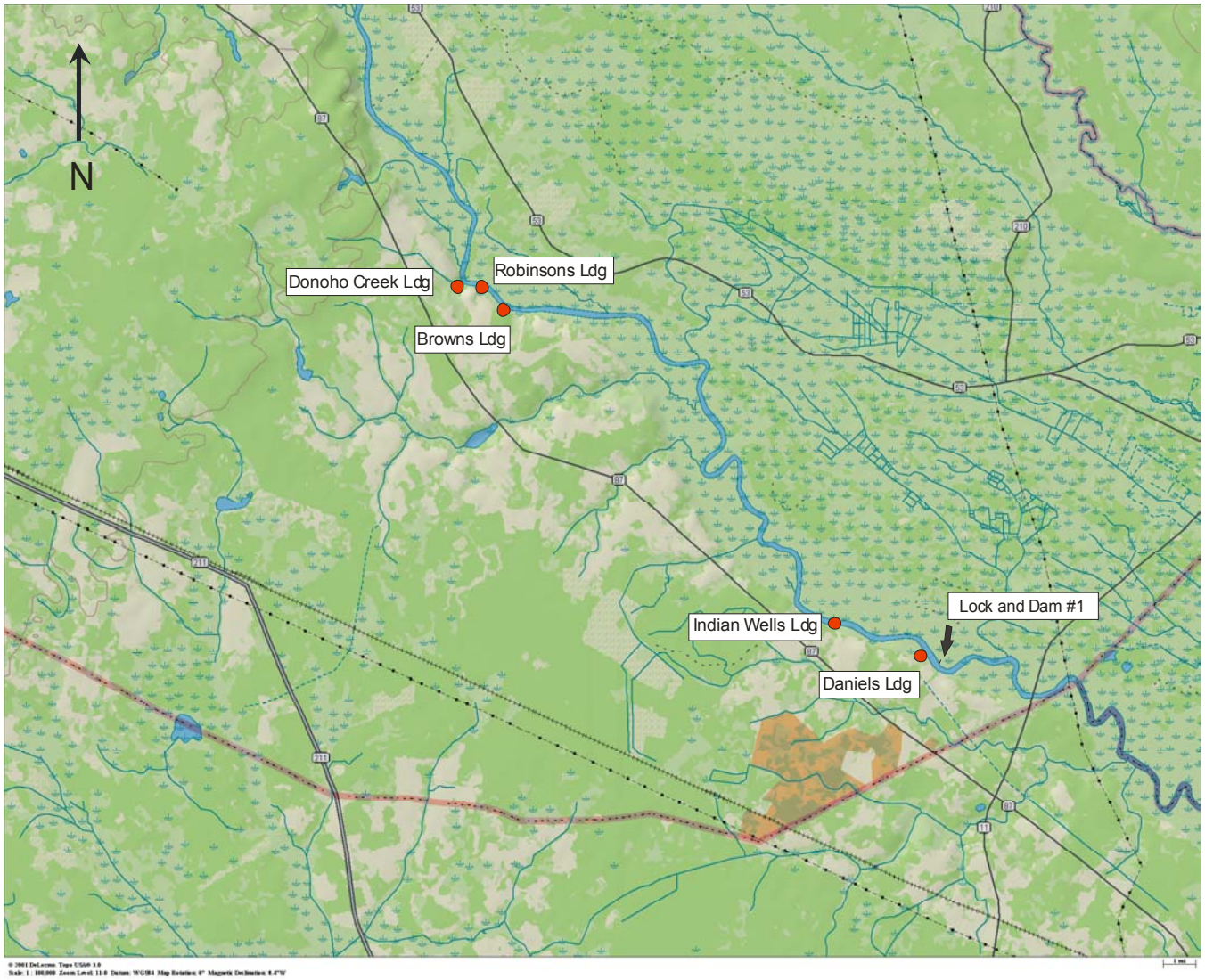

Figure 2a. Location map of Cretaceous outcrops upstream of Lock and Dam #1, Cape Fear River. See Farrell, et al, 2001, pp. 108-114, for outcrop descriptions.

Figure 2b. Location map of Cretaceous outcrops upstream of Lock and Dam #1, Cape Fear River. See Appendix 6 for outcrop locations.

coastal plain outcrops and lithologic similarity within and between units, detailed unit and boundary delineation was problematic. Earliest works (Stephenson, 1912, 1923) sought to define and correlate formations, whereas later studies built upon the existing framework and divided units into packages representative of depositional environment (Custer, 1981; Dockal et al., 1998; Farrell, 1998; Farrell, et al., 2001; Finneran, 1980; Heron, 1958; Heron and Wheeler, 1964; Prowell, et al., 2003; Sohl and Owens 1991; Swift, 1964, Swift and Heron, 1969). Owens (1989) published the Florence 1° x 2° quadrangle geologic map of the Cape Fear region.

Sohl and Owens (1991) subdivided the Upper Cretaceous section into three units based on lithologic differences: the Middendorf, Black Creek, and Peedee Formations. They elevated the Black Creek Formation to group status and defined three unconformity-bounded formations in the Black Creek: the Tar Heel, Bladen, and Donoho Creek (Fig. 3). Within the Upper Cretaceous, certain lithologies persist through one or more time periods and/or formation boundaries whereas others occur in only one type section or locality, outcrop, or corehole (Heron and Wheeler, 1964).

Sequence Stratigraphy

The application of sequence stratigraphic concepts may provide resolution to ambiguities in the understanding of Upper Cretaceous depositional systems in the Cape Fear region. These concepts are used to package sediments based on changes in sediment type, grain size, bed and bedset stacking patterns and relative position rather than by facies changes. Sequence stratigraphy began as a method of interpreting seismic reflection data in the petroleum industry (Vail et al., 1977) and contributed to the construction of a global cycle chart (Haq et al. 1987). These cycles were based on patterns of relative coastal onlap, correlated worldwide, and

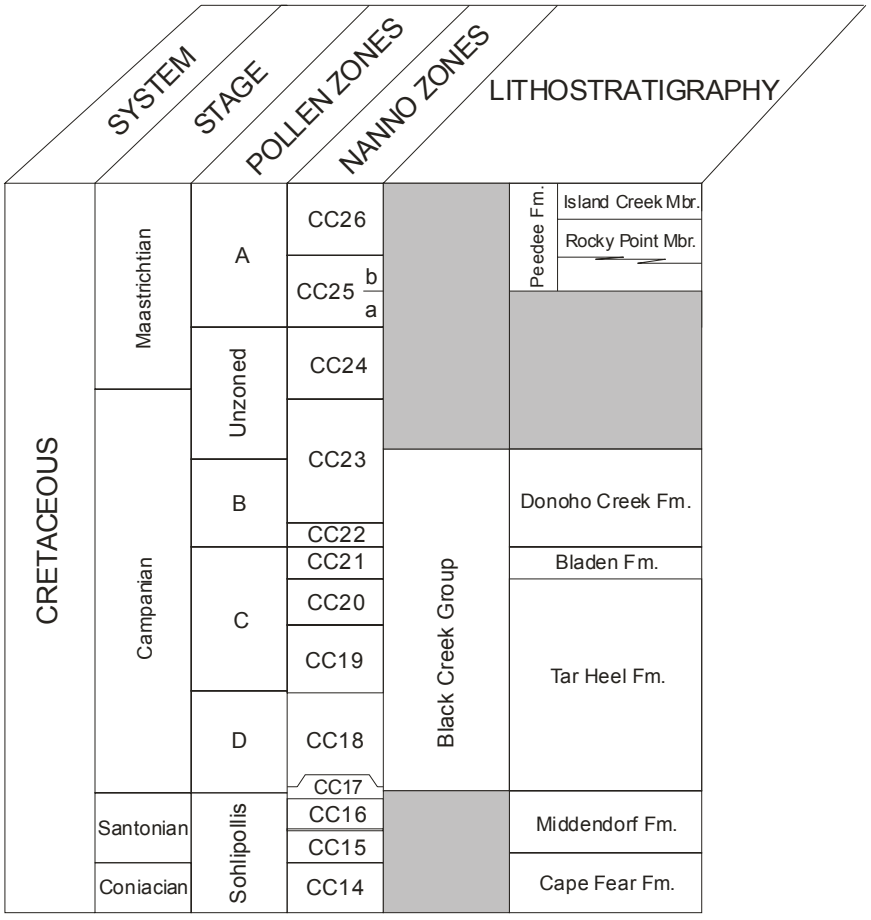

Figure 3. Cretaceous stratigraphy of southeastern North Carolina. Modified from Harris, pers. comm., 2003.

bounded by a series of widespread unconformities known as sequence boundaries. The stratigraphic sequence and its bounding surfaces are the basis of sequence stratigraphy (Miall, 1997). The depositional sequence is defined as, "a stratigraphic unit composed of a relatively conformable succession of genetically related strata, and bounded at its top and base by unconformities or their correlative conformities" (Mitchum et al., 1977, p.53). The bounding unconformities are thought to form by subaerial or submarine erosion (Type 1 and Type 2 boundaries, respectively) during periods of relative sea-level fall (Nummedal and Swift, 1987). Therefore, a depositional sequence is interpreted to represent a cycle of relative sea-level rise and fall (Vail et al., 1977).

Depositional sequences can be further subdivided into systems tracts, or three-dimensional, genetically related packages of lithofacies (Van Wagoner et al., 1988). A systems tract is deposited in response to a cycle, or portion of a cycle, of relative sea-level change (Mitchum et al., 1994) and is represented by shelf margin, lowstand, transgressive, or highstand deposits (Posamentier and Vail, 1988). The lowstand systems tract overlies the basal unconformity of a Type 1 sequence and the shelf margin systems tract the basal unconformity of a Type 2 sequence. Between the lowstand systems tract and the transgressive systems tract is the transgressive surface. This surface represents the critical marine transgression during a relative rise in sea level. On the continental shelf, the transgressive surface is frequently merged with the underlying sequence boundary (Van Wagoner et al. 1990). Separating the transgressive systems tract from the overlying highstand systems tract is the condensed section, which may contain a surface of maximum flooding. This surface is interpreted to represent the point within a sequence where sedimentation rates are low and the rate of sea level rise is maximum (Posamentier and Vail, 1988).

Although sequence stratigraphy began as a method for seismic interpretation, several studies demonstrate that sequence boundaries and systems tracts are recognizable in well logs and cores as well as in outcrop (Baum, 1986: Zullo and Harris, 1987; Nummedal and Swift, 1987; Zarra, 1989; Van Wagoner et al.1990; Mitchum et al., 1993, Miall, 1997).

METHODOLOGY

Sampling and Description

Field Exposures

The Donoho Creek and Peedee Formations are exposed in twelve outcrops on the south bank of the Cape Fear River (Figs. 2a and 2b). In general, Donoho Creek lithology is exposed upstream of Black Rock Landing (milepost 37), and the Peedee Formation is exposed downstream. Nine of these Upper Cretaceous exposures, from Donoho Landing (milepost 50.2) to Strawberry Hill (milepost 18.2), were visited. All exposures were described, and all sections downstream of Kings Bluff (milepost 38) measured and sampled. Although the samples were not included in laboratory analyses, the information gathered from field work aided in understanding the stratigraphic patterns found in the cores.

Core Sections

The U.S. Geological Survey drilled the Kure Beach core (latitude: 33º 58' 24" N., longitude: 77º 55' 01" W.) in the summer of 2001 to a depth of 1386 ft.; however, only the section between 467 ft. and 130.1 ft. was described and sampled (Fig. 5). This section was selected based upon preliminary analysis, as it spanned the interval from the Campanian/Maastrichtian to the Maastrichtian/Danian boundaries. The core is housed at the North Carolina Geological Survey Office in Raleigh, N.C. The Black Rock Landing (latitude: 34º 23' 45" N., longitude: 78º 16' 06" W.) and Hilton Park cores (latitude: 34º 15' 19" N., longitude 78º 56' 50" W.) are also U.S.G.S. core holes and were

a.

265.4 - 268.4 ft.

b.

403.0 - 406.0 ft

c.

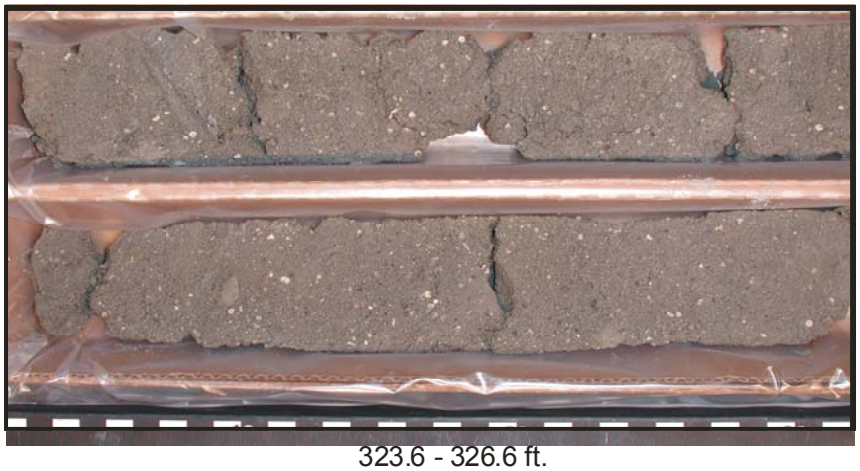

323.6 - 326.6 ft.

Figure 4. Selected Kure Beach cores illustrating; (a) bioturbation and burrow structures, (b) lithified horizons (at bottom left), and (c) allcohems (crinoid columnals). Note: Depths given are not continuous.

a.

b.

Figure 5. (a) Hilton Park and (b) Black Rock Landing cores.

both drilled in August of 1999. Total depth of the Black Rock Landing core is 52 ft.; the Hilton Park core is 62 ft. Cretaceous sediments are found in the Black Rock Landing core from the core base to 29 ft. (Fig. 5). In the Hilton Park core the Cretaceous section spans from the core base to approximately 26 ft. (Fig. 5). Both cores are housed at the University of North Carolina at Wilmington. Degree of induration, presence of megafossils, relative amount of bioturbation, lithology, and sedimentary structures were described in all three cores. The presence of bioturbation was identified through comparison to figures from Farrell, et al., 2001. Sediment colors were identified using the GSA rock color chart (The Rock Color Chart Committee, 1975). Supplemental descriptions for the Kure Beach core were obtained from the U.S. Geological Survey and integrated into descriptions made during core sampling.

Eighty samples were taken from the Kure Beach, ten from the Hilton Park, and nine from the Black Rock Landing cores. All cores were sampled at approximately 5 ft. (1.52 m) intervals, except near picked boundaries. In boundary areas, samples were taken approximately 1.5 ft. (0.46 m) above and below the contact. One-quarter round was taken for laboratory analysis and most samples measured 0.2 ft. (0.06 m) in length. The outside of each core sample was gently scraped to remove contaminants from other parts of the well bore prior to placement into sample bags.

Laboratory

Samples were disaggregated and dried in a 40° C oven for 2 hours, or until no moisture remained. Between 14 and 16 g of sample were digested using 20 percent HCl, following the methods of Ireland (1977). When digestion was complete the samples were filtered, dried in a 40°C oven and weighed. A solution of distilled water and 40 g/L Calgon® was added to the

residues to disperse mud. The samples were wet-sieved using a U.S. Standard No. 230 screen (62μm). Sediment retained on the No. 230 screen was dried and weighed (Appendix 1).

The sand fractions, ranging in weight from 1.1g to 12.9g, were dry-sieved at whole-phi intervals using an ATM Model L3P Sonic Sifter. Each sample was sieved for five minutes. The fractions remaining on each sieve were weighed using a calibrated Metler scale. Data were entered into GRANPLOTS (Basillie, 2002), and Folk and Ward (1957) grain size statistics calculated.

Mineralogical Analysis

Dry-sieved samples were examined using a Nikon® type 104 binocular microscope. Volume percentages of quartz, glauconite, phosphate, mica, iron oxides, and heavy minerals were estimated through comparison to visual charts representing 10%, 20%, 30% and 40% of glauconite mixed with quartz sand. Additional notes were made on degree of sorting, rounding, preservation of fossils, types of minerals, and the presence of frosting or staining. Percentages of abundance were grouped into the following categories: 0-1% Trace, 1-15% Rare, 16-25% Common, 26-50% Abundant, 51-75% Very Abundant, and >75% Dominant (Appendix 3). In addition, original sample splits were examined from the Kure Beach core hole in order to determine the types of allochems present and estimate their percentage. The splits were taken from sections of the core where no materials were thin sectioned. Silt and clay were decanted from the sediment and the major allochems were classified using the same abundance categories as in the mineralogical examinations.

Thin Section Analysis

Thirteen indurated or semi-indurated samples were sent to Arizona Quality Thin Sections, Inc.,for thin-section preparation; where necessary, samples were impregnated with blue dye. Samples were analyzed using a Zeiss photomicroscope. Two hundred points were counted

per thin section using a mechanical stage. Micro- and megafossils were identified to the family level. Lithology, relative abundance of minerals, biogenic structures, bedding, laminations, and degree of dissolution or recrystallization were described (Appendix 4).Sequence Stratigraphic Analysis

Lithologic successions in all three cores were grouped, using sequence stratigraphic concepts, into genetically related packages bounded by unconformities. Unconformities were tentatively identified by using classic characteristics such as irregular surfaces overlain by conglomerate, abrupt changes in lithology, or in stratal stacking patterns (i.e., aggradation, progradation, retrogradation. See Van Wagoner et al., 1988 for further details). Further analysis refined the originally picked genetically related packages into four depositional sequences, bounded by regional unconformities. Results below discuss core geology using informal sequences designated by numbers with the lower number representing the oldest sequence and the higher number the youngest.

RESULTS

Kure Beach Core

Sequence 1

Sequence 1 is first recognized at 467 ft. and ends at an unconformity at 410 ft. The sequence is characterized by unconsolidated, massively bedded, mottled olive gray (10YR 6/2 and 10YR 4/2) calcareous sand (Fig. 6). Weight percent insoluble residue averages 73.5% (51.2% sand, 22.3% silt and clay). Mean grain size of the sand fraction is 1.82 φ (medium sand) and the sand-sized sediments are moderately sorted (0.80 φ), subangular, coarse-skewed (0.12) and very leptokurtic (2.78). Quartz is the main mineral constituent, but two glauconite-rich

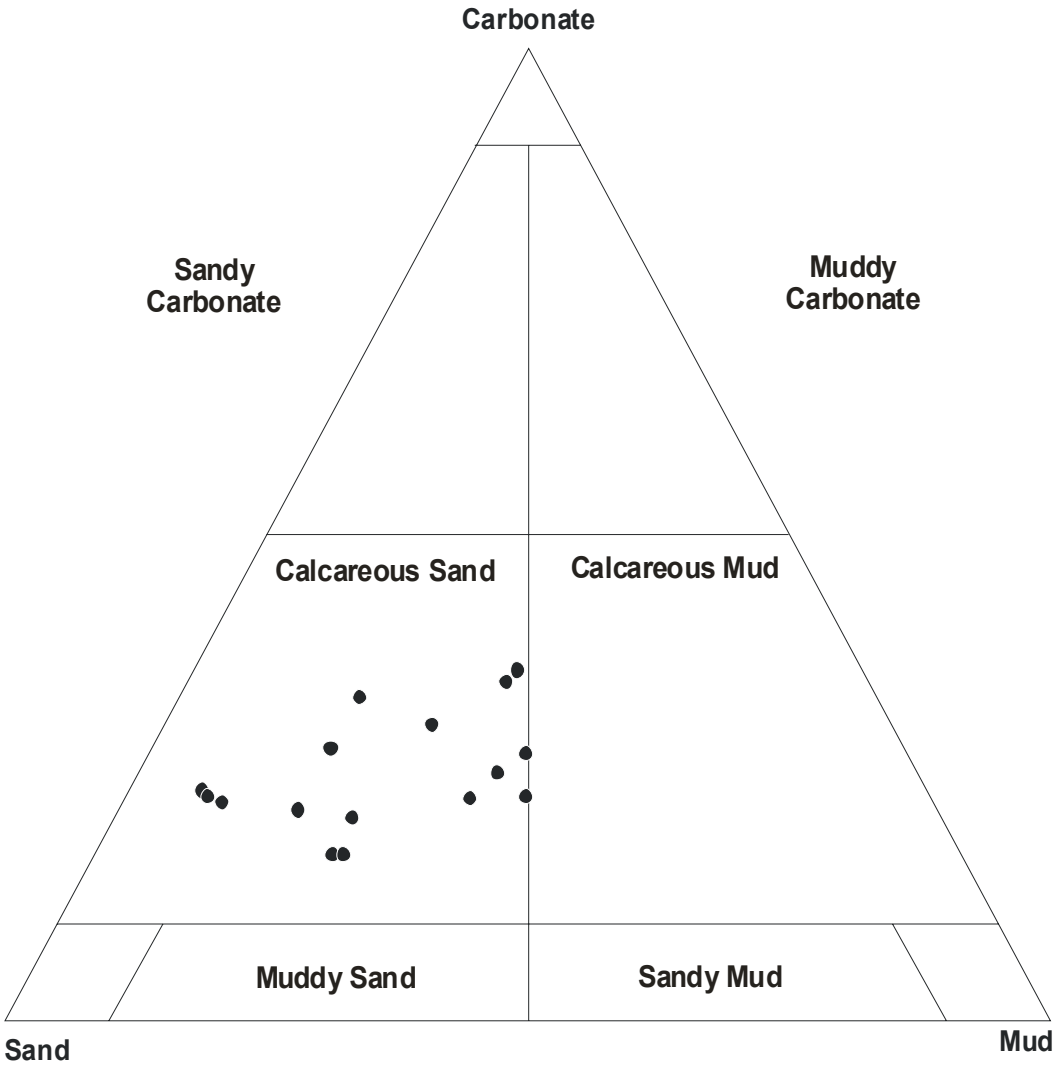

Figure 6. Sequence 1 lithology in the Kure Beach core. Fields after Lindholm (1987). Note: For all ternary diagrams, each symbol represents an individual sample

horizons are present at 443 ft. and 430 ft. Phosphate, muscovite, pyrite, heavy minerals, and lithoclasts are found in trace amounts. The lithoclasts are generally medium- to coarse sand size and are composed of silt-sized grains of quartz, glauconite, phosphate and mica aggregated with quartz cement.

Due to the unconsolidated nature of the sediments of Sequence 1 no thin sections were made. Major allochems identified during microscopic examination included unidentifiable mollusk fragments as well as benthic and planktonic Foraminifera.

The first sequence boundary, SB-1, marking the top of Sequence 1, is characterized by a highly irregular surface as well as a color change from olive gray (10YR 6/2 and 10YR 4/2) to darker greenish gray (5GY 2/1 and 5Y 4/1). Rip-up clasts were observed above the boundary between 405 and 400 ft. Grain size fines abruptly from 1.49 φ (upper medium sand) below the boundary to 2.47 φ (lower fine sand) above.

Sequence 2

Sequence 2 begins above the unconformity at 410 ft. and is bounded at its top by a second unconformity at 318 ft. This sequence is significantly thicker than Sequence 1 and varies in lithology. At its base, Sequence 2 is lithologically similar to Sequence 1. The basal section is characterized by unconsolidated, massively bedded, greenish gray (5GY 2/1 and 5Y 4/1) calcareous sand (Fig. 7). Weight percent insoluble residue averages 71.8% (49.5 % sand, 22.3% mud) and mean sand size is 2.47 φ (fine sand). The sand fraction is moderately sorted (0.91 φ), subangular to subrounded, near symmetrical (-0.05), and very leptokurtic (2.46). Quartz is the most abundant mineral and glauconite content decreases slightly away from the basal unconformity. Relative abundance of phosphate and mica increases slightly as glauconite decreases. No samples from the base of Sequence 2 were thin sectioned, but mollusk fragments,

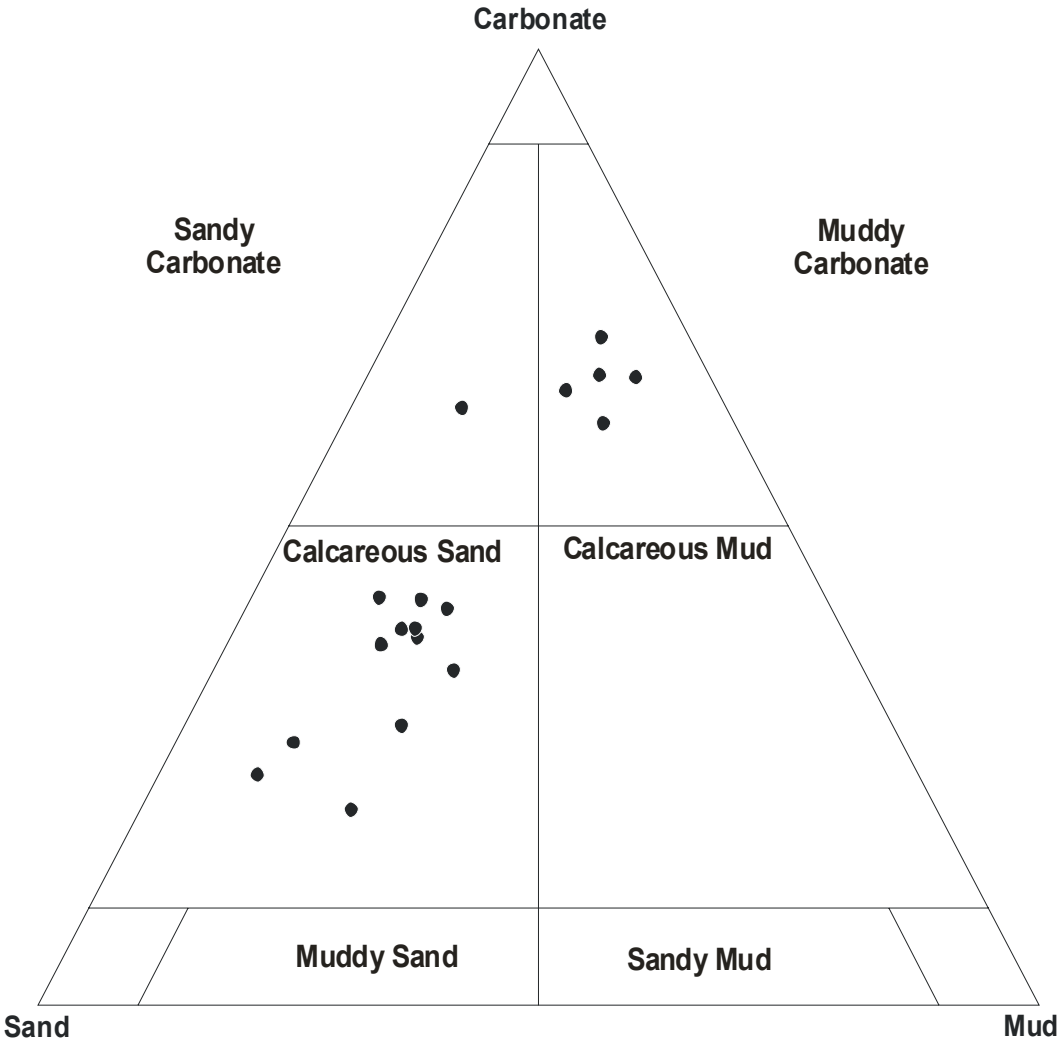

Figure 7. Sequence 2 lithology in the Kure Beach core. Fields after Lindholm (1987).

crinoid columnals and foraminifers are the major allochems identified by binocular microscopic examination.

Above the basal calcareous sand a lithified horizon marks the transition to midsection muddy carbonate (Fig. 7). The basal and midsection sediments are similar in color (mottledolive-gray, 5Y 4/1 and 5Y 3/2), but in the midsection, weight percent insoluble residue decreases to 35.1% (11.5% sand, 23.6% mud) and mean sand size decreases to 2.92 φ (fine sand). The sand is moderately sorted (0.98 φ), subangular, fine-skewed (0.15) and very platykurtic (0.66). Quartz forms the majority of the mineral assemblage; relative abundance of glauconite, phosphate and muscovite decrease slightly from the section below. Heavy minerals and pyrite are found in trace amounts in a few samples. An indurated horizon separating the two lithologies was thin-sectioned (Fig. 8). Allochems identified in the thin section include crinoids, mollusk and echinoid fragments, ostracodes and both benthic and planktonic Foraminifera.

The upper extent of Sequence 2 is characterized by a gradational change in lithology from muddy to sandy carbonate, and then to calcareous sand (Fig. 7). Sediment color is similar to that of the underlying sediments (5Y 4/1 and 5Y 6/1) and is mostly massive, friable and indistinctly mottled. Mean weight percent insoluble residue increases to 55.0% (41.2% sand, 13.8% mud), with the mud generally restricted to thin laminations. The sand fraction coarsens slightly to 2.63 φ (fine sand) and is moderately well-sorted (0.70 φ), subangular to subrounded, strongly coarse-skewed (-0.39) and extremely leptokurtic (3.35). Mineralogically, quartz is most abundant and glauconite, phosphate and mica are present in small amounts. Traces of pyrite, lithoclasts and heavy minerals are found in a few samples.

Three lithified horizons that occur in the upper part of Sequence 2 were thin-sectioned. Allochem types are similar in the middle and upper sections of the sequence, but in the upper

a.

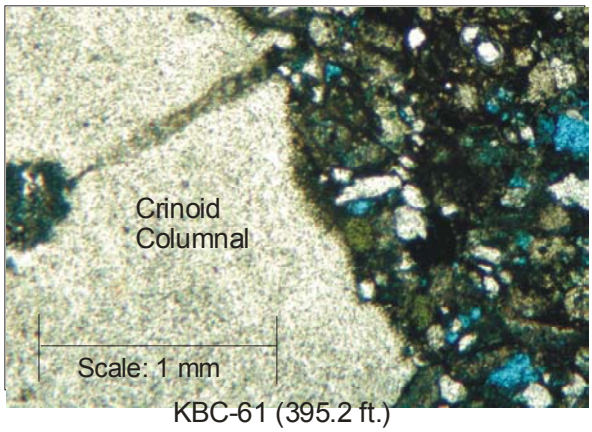

KBC-61 (395.2 ft.)

b.

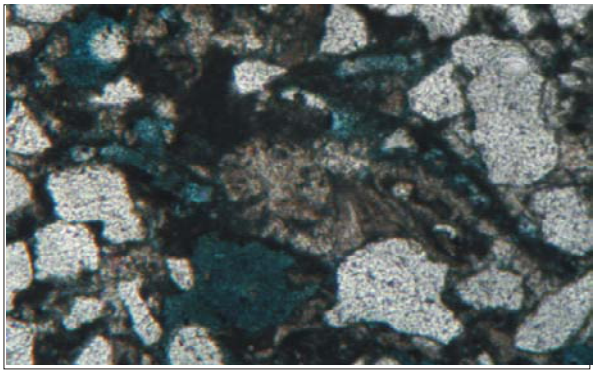

KBC-23 (224.9 ft.)

c.

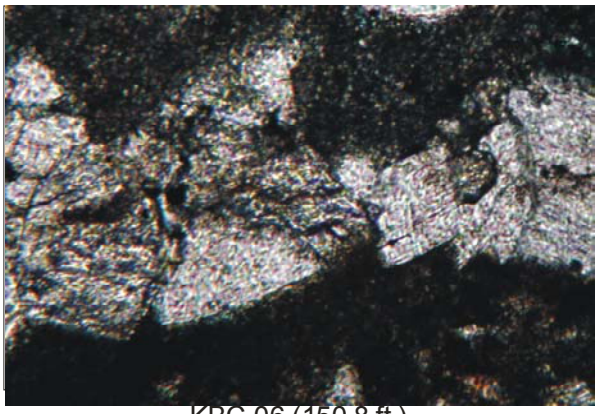

KBC-06 (150.8 ft.)

Figure 8. Thin sections taken from the Kure Beach core. (a) Deeper samples are characterized by blocky calcite spar, high matrix percentages, and allochems such as crinoid columnals. (b) Samples from midsection intervals often contain large, rounded quartz grains in a dirty, bioturbated, micrite matrix. (c) The highest sample thin-sectioned contains abraded and corroded dolomite rhombs. Note: Photos are of equal scale.

section relative abundance of crinoid columnals increases. Other allochems include benthic and planktonic Foraminifera, mollusk and echinoid fragments and ostracodes. In one sample, mollusk fragments could be identified as gastropods (see Appendix 4).

Sequence 3

Sequence 3 begins at an unconformity at 318 ft. and ends at an unconformity at 152 ft. This sequence spans nearly half of the described core section and is characterized by a variety of lithologies (Fig. 9) and sedimentological features. The base of the sequence is defined by an increase in mud and the absence of crinoid columnals. The basal unconformity is also marked by a change in color from olive gray (5Y 4/1) to light gray (N8) and a change from friable to indurated sediments. Moving upward from the unconformity, Sequence 3 is characterized by calcareous sand grading to calcareous mud. Bedding is generally massive, indistinctly mottled and marked by alternating zones of indurated and friable sediments. Mean weight percent insoluble residue is 67.2% (35.2% sand, 32.0% mud). Mean sand size is 2.78 φ (fine sand) and the sand fraction is moderately sorted (0.81 φ), subangular, strongly coarse-skewed (-0.54), and extremely leptokurtic (3.52). Quartz is the most abundant mineral, but glauconite is concentrated in a few intervals at the base of the sequence. Phosphate and muscovite are present in all samples, and heavy minerals are virtually absent.

No materials were thin-sectioned from the base of Sequence 3, but binocular microscopic examination suggests mollusk and echinoid fragments and benthic Foraminifera are the main allochems present.

Sequence 3 grades to a dark olive gray (5Y 3/1) to olive gray (5Y 4/1) muddy carbonate. Bedding is generally massive but clay laminations are present, as are zones of diagenetic concretions, which are generally lighter in color (5Y 8/1). Biogenic structures are more distinct

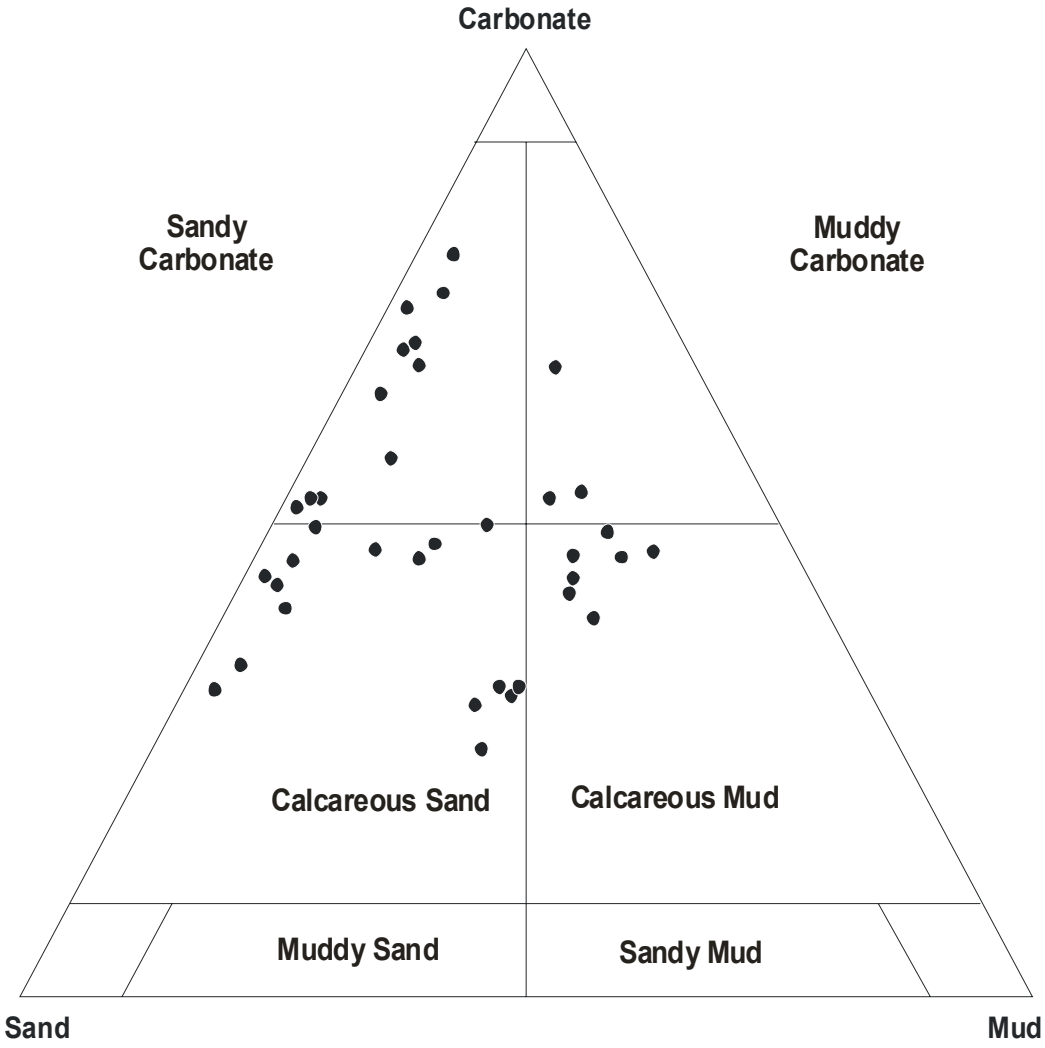

Figure 9. Sequence 3 lithology in the Kure Beach core. Fields after Lindholm (1987).

and are often iron stained. Mean weight percent insoluble residue decreases to 45.2% (19.6% sand, 35.6% mud). Mean grain size of the sand fraction fines to 3.12 φ (very fine sand). The sand is moderately well-sorted (0.57 φ), subangular, strongly coarse-skewed (-0.41) and leptokurtic (1.50). Quartz is again the most abundant mineral. Glauconite, phosphate and muscovite are found in all samples. Heavy minerals, pyrite and lithoclasts are found in isolated areas.

No materials were thin sectioned from the midsection of Sequence 3, but microscopic examination of core splits found mollusk and echinoid fragments and benthic Foraminfera to be the main allochems present.

The upper 100 ft. of Sequence 3 are characterized by a coarsening of sediments from a dark olive-gray (5Y 3/1) muddy carbonate to an olive gray (5Y 4/1) sandy pelecypod mold grainstone to light olive gray (5Y 6/1) and dusky yellow and (5Y 6/4) calcareous sand. Several lithified zones are found in the uppermost part and are sites of shell concentration. Mean weight percent insoluble residue is 45.7% (38.4% sand, 7.3% mud). The sand fraction coarsens upward from 2.64 φ (fine sand) to 1.64 φ (medium sand), becomes more well-sorted (0.55 φ to 0.69 φ), ranges from subangular to rounded, is near symmetrical (0.02) and very leptokurtic (2.29). Quartz is the dominant mineral throughout the section. Glauconite, phosphate, muscovite, pyrite, and heavy minerals decrease to trace amounts upsection. Some of the highest samples within Sequence 3 also contain silicified shells.

Eight samples were thin-sectioned from materials in the upper part of Sequence 3. Faunal assemblages shift from dominantly foraminiferal at its base to mollusk fragment dominant at its top. Benthic Foraminifera are present in all samples, but planktonic foraminifers

are absent in higher sediments. Echinoid fragments and ostracodes are found in most samples, and one sample also contains fragmented bryozoans and gastropods.

Sequence 4

Sequence 4 is the youngest sequence of the Kure Beach core examined. It begins at 150 ft. and is last described at 130 ft. The upper part of the sequence is not included in this study because it is interpreted to be Paleocene in age. Sequence 4 is characterized at its base by a dissolution surface overlain by yellowish gray (5Y 8/1) wackestone. The remainder of the sequence is unconsolidated olive gray (5Y 4/1) to olive black (5Y 2/1), massively bedded, bioturbated sand and calcareous mud (Fig.10). Weight percent insoluble residue varies greatly, but averages 74.9% (50.2 % sand, 24.7% mud). The sand fraction has an average grain size of 2.19 φ (fine sand), is poorly sorted (1.02 φ), subangular to subrounded, fine-skewed (0.23), and very leptokurtic (2.09). Quartz is the most abundant mineral, but glauconite content is high in isolated areas. A thin section taken from the base of Sequence 4 also contains dolomite rhombs (Fig. 8c). Phosphate and muscovite increase above the boundary between sequences, and heavy minerals and silicified shells occur in some samples.

Hilton Park Core

Sequence 1

Sequence 1 in the Hilton Park core is first identified at core base (62 ft.) and ends at 47 ft. It is characterized by alternating intervals of pale olive (10 Y 6/2), massively-bedded calcareous sand and light olive gray (5Y 5/2) sandy, pelecypod-mold grainstone (Fig. 11). Mean weight percent insoluble residue is 61.8% (42.3% sand, 9.5% mud). Average grain size of the sand fraction is 2.42 φ (fine sand) and the grains are moderately well-sorted (0.52 φ), angular to subrounded, coarse-skewed (-0.16), and extremely leptokurtic (4.52). Quartz is the most

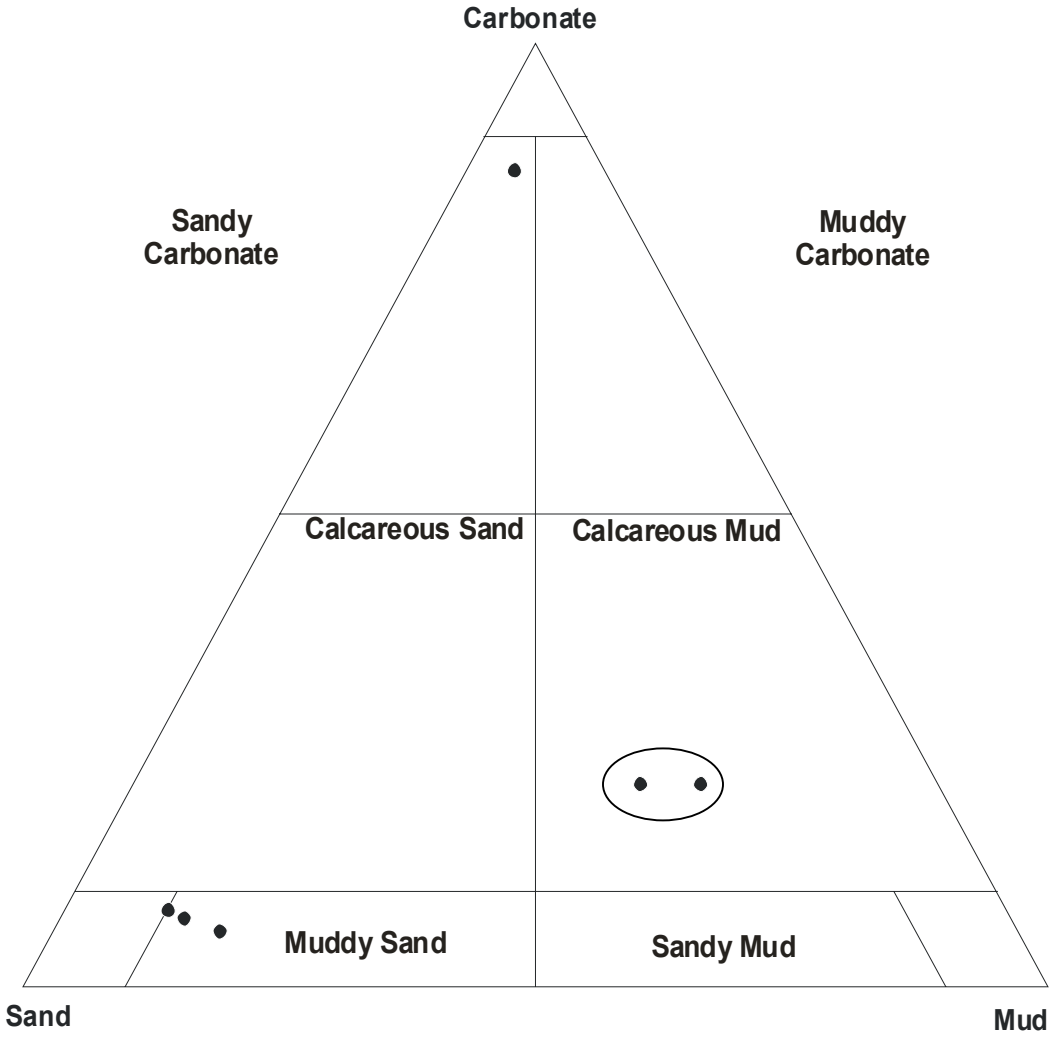

Figure 10. Sequence 4 lithology in the Kure Beach core. Samples interpreted to be Paleocene in age are circled. Fields after Lindholm (1987).

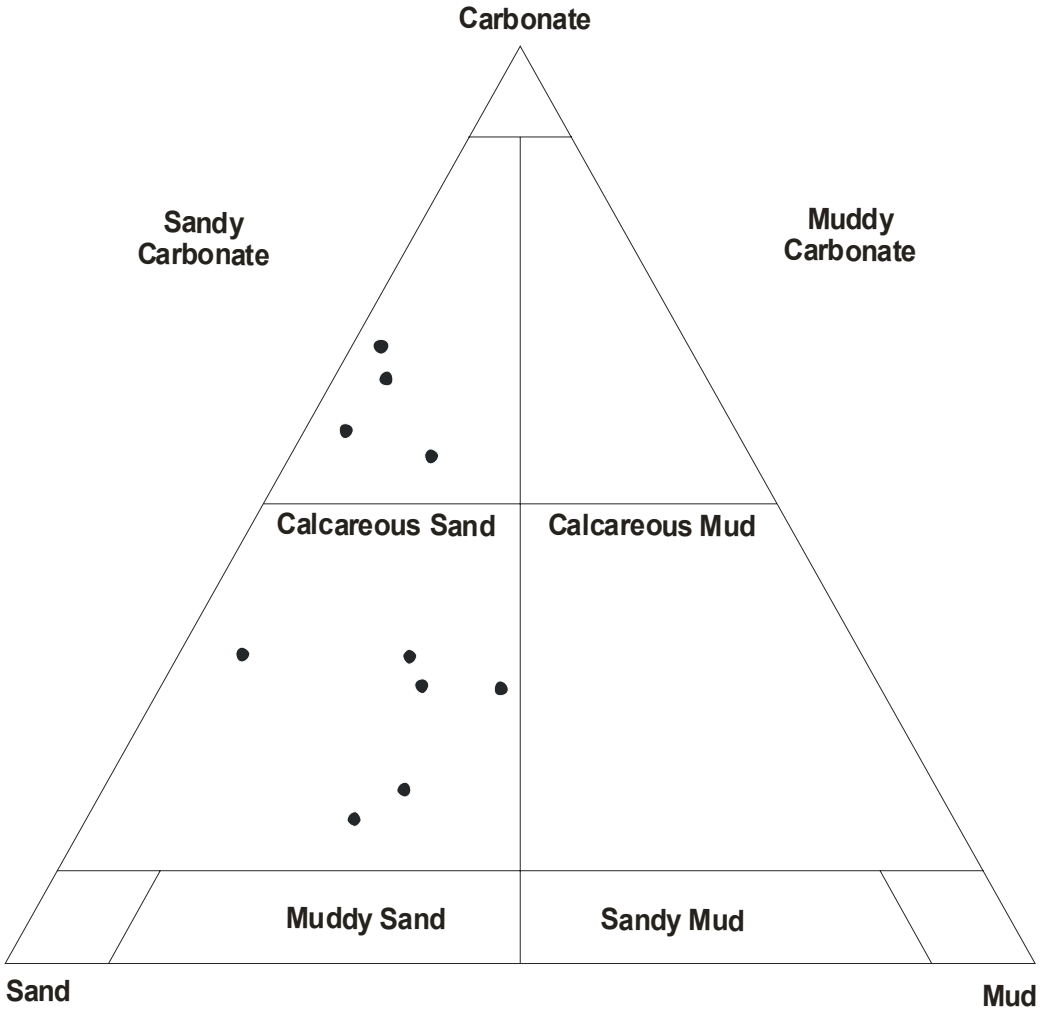

Figure 11. Sequence 1 and 2 lithology in the Hilton Park core. Fields after Lindholm (1987).

abundant mineral present, with glauconite, phosphate, muscovite, silicified shells and heavy minerals present in small amounts. Major allochems include mollusk fragments and disarticulated mollusks, bryozoans, ostracodes, and benthic Foraminifera.

Sequence 2

Sequence 2 extends from 44 ft. to approximately 26 ft. Although there is a 2 ft. loss of section below the upper boundary, the gamma ray and core logs suggest a distinct unconformity at this depth. The sequence is characterized by dark greenish gray (5G 4/1), massively bedded, unconsolidated, calcareous sand (Fig.11). Mean weight percent insoluble residue increases to 67.03% (42.95% sand, 24.18% mud). Mean sand size is 2.81 φ (fine sand) and the sand fraction is moderately well-sorted (0.65 φ), subangular to subrounded, coarse-skewed (-0.13), and very leptokurtic (2.41). Quartz is the most abundant mineral, with relative percentages of glauconite, phosphate, muscovite, pyrite and heavy minerals increasing from the previous sequence. No silicified shells are present in this sequence. Major allochems are mollusk fragments, occasional small, disarticulated, unidentifiable mollusk valves (~1 in.) and benthic Foraminifera.

Black Rock Landing Core

Sequence 1

Sequence 1 begins at core base (54 ft.) and ends at an unconformity at 41 ft. It is characterized by massively bedded, bioturbated, mottled greenish-, olive-, and grayish-black (5 GY 2/1, 5Y 2/1, and N2, respectively), friable to unconsolidated calcareous sand (Fig. 12). Also present in this sequence are indurated olive gray (5Y 4/1), rounded concretionary masses, one to two inches in diameter, that appear to be zones or lenses of shell concentration. Mean weight percent insoluble residue for this sequence is 74.4% (59.5 % sand, 24.9% mud). The

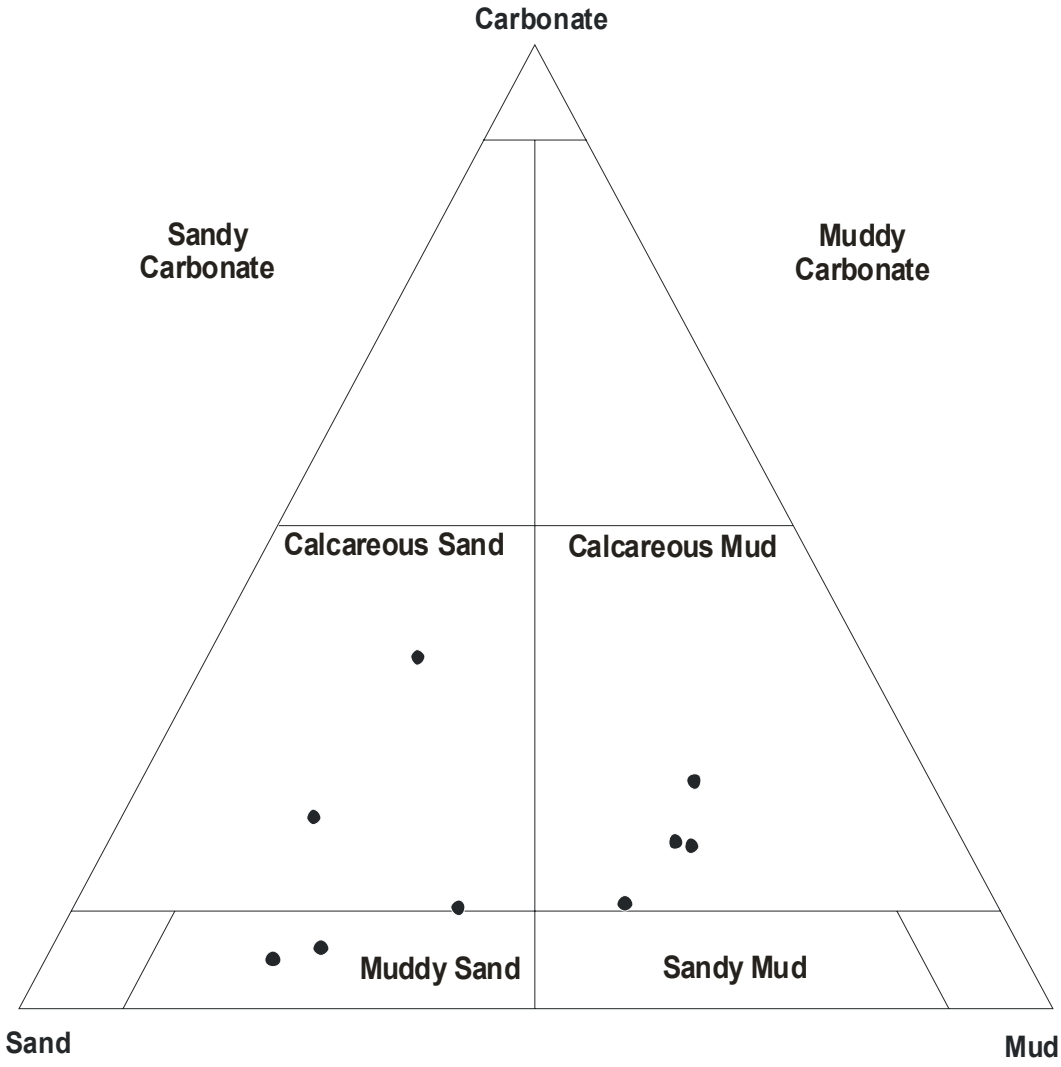

Figure 12. Sequence 1 and 2 lithology in the Black Rock Landing core. Fields after Lindholm (1987).

sand fraction has an average grain size of 1.78 φ (medium sand), is moderately sorted (0.93 φ), subangular, near symmetrical (-0.07), and very leptokurtic (2.52). Quartz is the most abundant mineral and glauconite, phosphate, muscovite, pyrite and heavy minerals are present in all samples. Mollusk fragments and benthic Foraminifera are the dominant allochems.

Sequence 2

Sequence 2 begins above the unconformity at 41 ft. and ends at 29 ft. The sequence is characterized by massively bedded and bioturbated, unconsolidated, greenish black (5 GY 2/1) calcareous mud (Fig. 12). Mean weight percent insoluble residue measures 82.9% (28.3% sand, 54.6% mud). Mean sand size measures 3.24 φ (very fine sand) and the sand fraction is moderately well sorted (0.52 φ), subangular, strongly coarse skewed (-0.48), and extremely leptokurtic (2.80). Relative abundance of quartz decreases above the unconformity. Glauconite, phosphate, muscovite, pyrite, and heavy mineral percentages all increase in the younger sequence. Allochems include benthic Foraminifera and trace amounts of mollusk fragments.

SEQUENCE STRATIGRAPHY

Kure Beach Core

Sequence 1

Sequence 1 (467 ft – 410 ft.) is interpreted to represent two parasequences within the remnants of a highstand deposit (Fig.13). The first parasequence averages more insoluble residue and the second averages more mud. Both parasequences are represented by coarse sediments that were deposited when rates of accommodation were low and outpaced sediment supply (Emry and Myers, 1996). In the oldest parasequence, sediments coarsen upward to 443 ft., at which point glauconite content increases sharply. Glauconite continues to represent

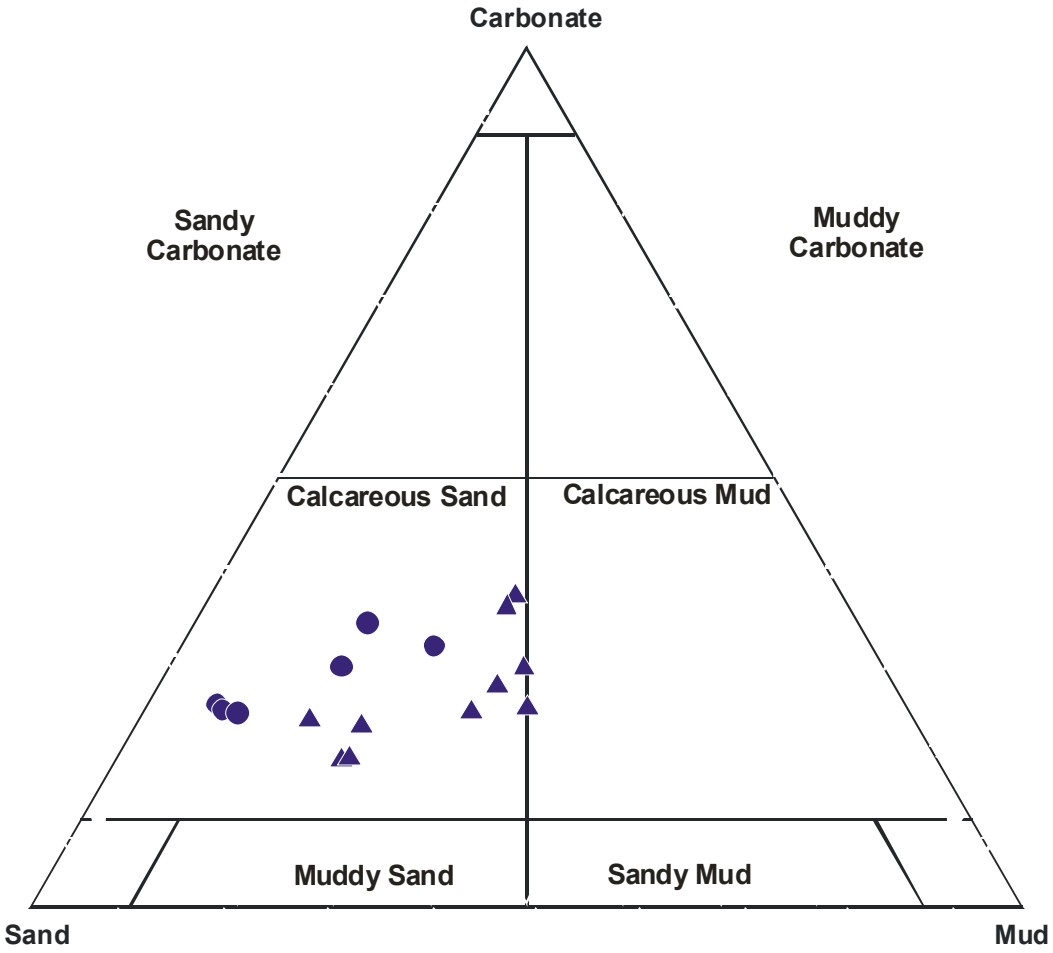

Figure 13. Comparison between the lithologies of parasequence 1 (triangles) and parasequence 2 (circles), Sequence 1, Kure Beach core. Fields after Lindholm (1987).

Table 1. Characteristics of Sequence 1, Kure Beach core

Kure Beach Core Description	**Parasequence 1**	**Parasequence 2**
Depth (ft.)	467-442	442-410
Color	olive-gray	olive-gray
Lithology	calcareous sand	calcareous sand
Bedding	massive/ bioturbated	massive/ bioturbated
Induration	unconsolidated	unconsolidated
Quartz	C-D	C-D
Glauconite	R-VA	R-D
Phosphate	T	T
Mica	T	T-R
Crinoids	-	-
Mollusks	R	R
Benthic Foraminifera	R	R
Planktonic Foraminifera	R	R
Sedimentological Characteristics of Sampled Population		
Carbonate (mean wt. %)	24.7	26.8
Terrigenous Fraction (mean wt. %)		
Percent Gravel	0	0
Percent Sand	46.4	59.1
Percent Mud	29.0	14.1
Mean grain size (φ)	1.85 (lower medium sand)	1.79 (lower medium sand)
Sorting (φ)	0.85 (moderately sorted)	0.72 (moderately sorted)
Skewness	0.12 (coarse-skewed)	0.07 (near symmetrical)
Kurtosis	2.61 (very leptokurtic)	3.05 (extremely leptokurtic)
Roundness	subangular	subangular

Index: D = Dominant (>75%) VA = Very Abundant (51-75%) A = Abundant (26-50%)
C = Common (15-25%) R = Rare (1-15%) T = Trace (<1%) - = Not observed

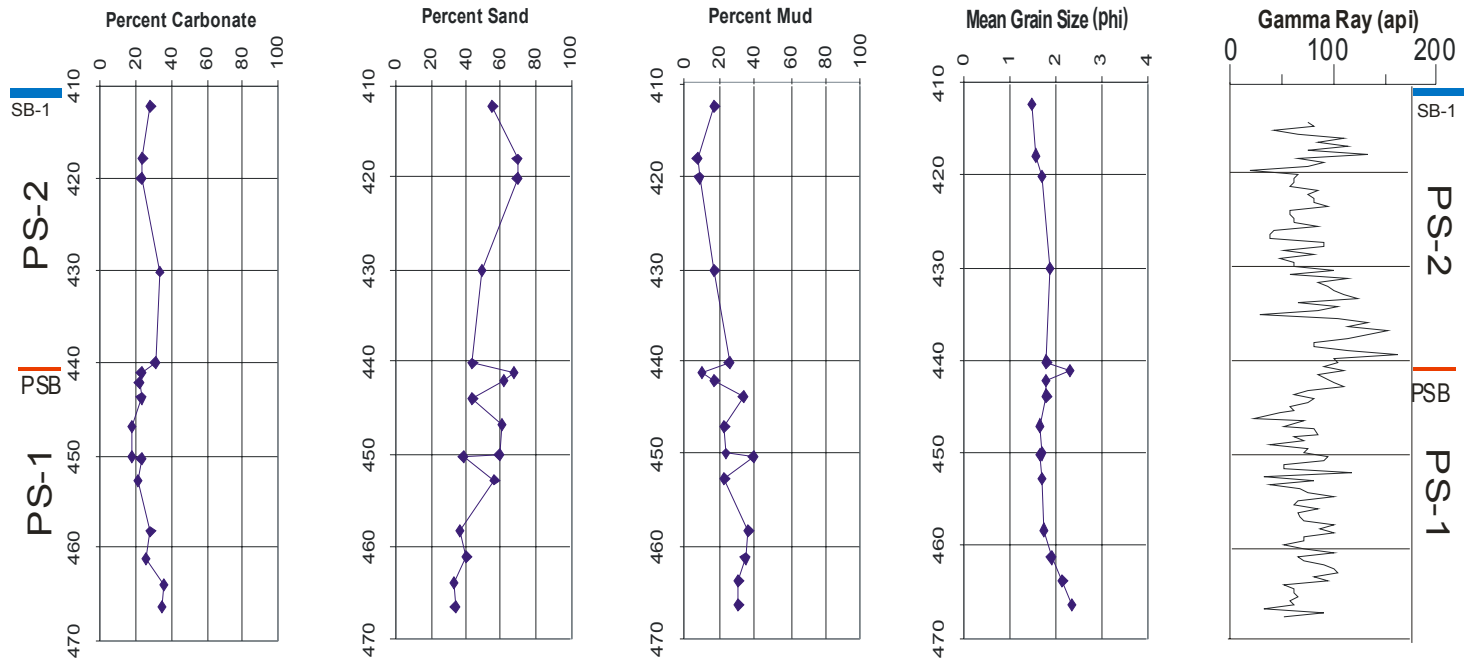

Figure 14. Graphical representation of Sequence 1 lithology in the Kure Beach core. Along each vertical axis is core depth in feet. PS = parasequence, PSB = parasequence boundary, SB = sequence boundary.

greater than 25% of the sand fraction until the top of the sequence. The high authigenic mineral content indicates a flooding surface separates the two parasequences just below 440 ft. The second parasequence continues to coarsen upward, suggesting that sedimentation continued to outpace accomodation in the later highstand.

This stacking pattern is also evidenced on the gamma ray (GR) log (Fig. 14). The first parasequence gradually becomes more radioactive on the GR upsection just prior to 440 ft. At this point, the GR moves right due to the high glauconite content and the decrease of mud upsection. The second parasequence shows a similar GR signature. It begins with a sharp spike to the right above 440 ft. and then becomes slightly less radioactive upsection as glauconite content gradually decreases.

The uppermost extent of Sequence 1 is bounded by a distinct unconformity. The unconformity is evidenced by a highly irregular surface, a change in sediment color, and the first appearance of a lithified horizon. The unconformity is also constrained by biostratigraphic data (Jean Self-Trail, pers. comm., 2003). Sequence 1 contains calcareous nannofossils assignable to zone CC23, identified at a depth of 414 ft. Nannofossils assignable to zones CC24 and CC25a are absent in the core. Nannofossils indicative of zone CC25b are found at a depth of 400.2 ft. These data suggest S-1 is Campanian in age, and that sediments above 410 ft. are Maastrichtian in age (Fig.3).

A Type-1 sequence boundary separates Sequence 1 from Sequence 2 at a depth of 410 ft. This boundary is thought to have formed sometime in the late Campanian/ early Maastrichtian by the lowering of sea level and creation of a subaerial erosion surface. An approximate 5 million year hiatus separates the two sequences. This hiatus spans the duration of one entire cycle of transgression and regression (Fraser, 1989), so it is difficult to ascertain the events surrounding

the unconformity and underlying highstand. A considerable volume of sediment may have been removed during the lowering of relative sea level and much of the shelf area may have been subaerially exposed (Miall, 1997). The hiatus is further evidenced by the absence of calcareous nannofossil zones CC23 and CC24 offshore on the Blake Plateau and as far inland as Burches Ferry, South Carolina (Self-Trail, 2001; Self-Trail and others, 2002, respectively).

Sequence 2

Sequence 2 (410 ft. – 318 ft.) is interpreted to contain a thin lowstand wedge (LSW), a thin transgressive deposit (TST) and a thicker highstand deposit (HST) (Fig. 15). The LSW (410 ft. – 400 ft.) is characterized by fine-grained sand, most likely derived from reworking of highstand deposits of the previous sequence (Van Wagoner et al., 1988). The top of the lowstand wedge is marked by a coarser, slightly dirty, lithified horizon (400 ft.), identified as the transgressive surface. This horizon is characterized by a grainstone with in-situ diagenetic alteration and void-precipitated blocky calcite spar that is meteoric in origin. Some silicification is present on the edges of allochems, specifically echinoid fragments. Large Foraminifera, mollusk fragments and crinoid columnals are also present. A surface of maximum flooding at 384 ft. tops the thin transgressive deposit of fine-grained muddy carbonate. The maximum flooding surface shows increased amounts of authigenic sediments such as glauconite and phosphate above it.

The transition from the TST to HST is also evidenced by a switch from a retrogradational to a progradational stacking pattern (Miall, 1997). Grain size gradually coarsens upward and lithified horizons are common in the HST (Fig. 16). Average thickness of horizons is about 1 ft. The transition from consolidated to lithified sediments is usually gradual and bioturbation is more apparent in lithified horizons. From the TST to HST carbonate and clay content decrease

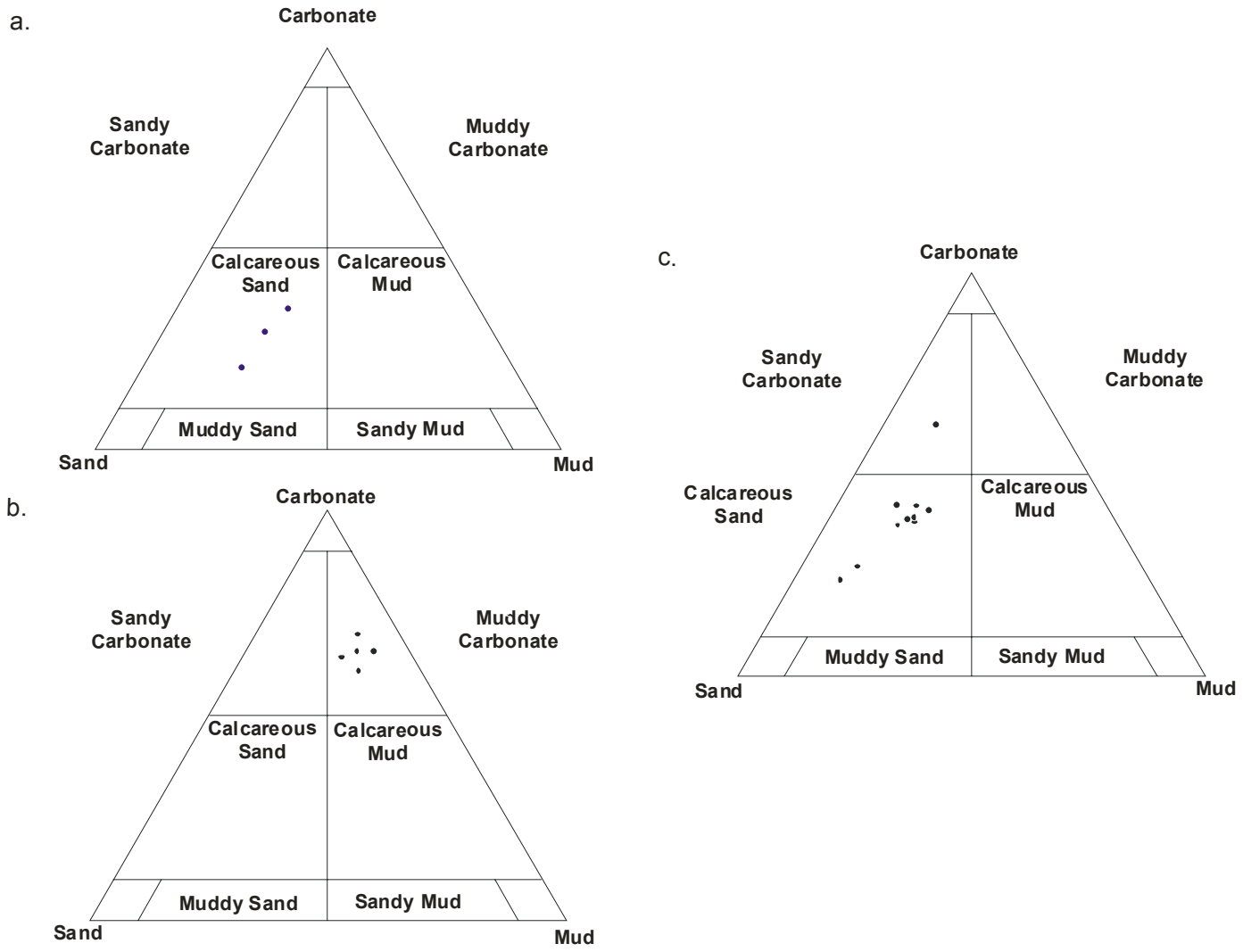

Figure 15. Lithologic comparison between systems tracts in Sequence 2 (a) lowstand wedge (LSW), (b) transgressive deposits (TST), (c) highstand deposits (HST), Kure Beach core. Fields after Lindholm (1987).

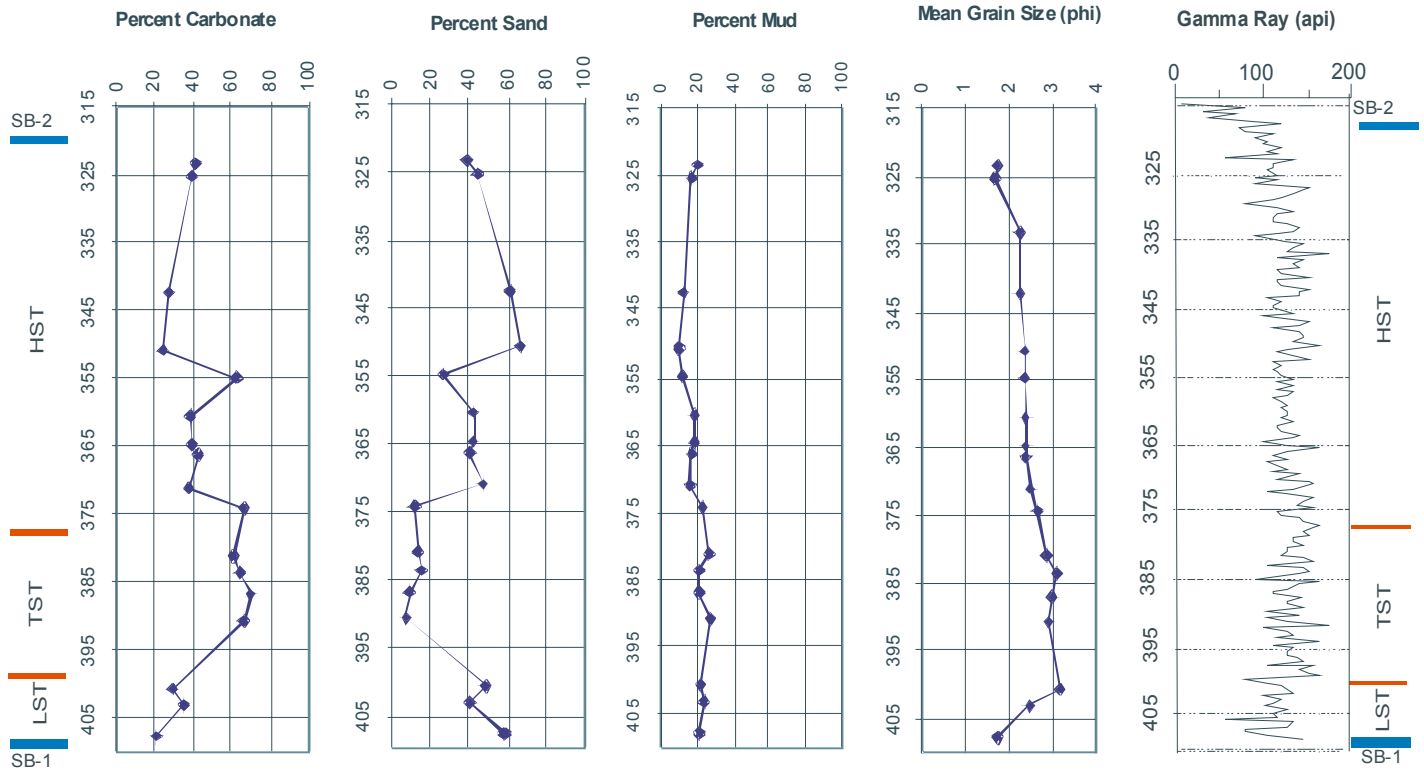

Figure 16. Graphical representation of Sequence 2 lithology, Kure Beach core. Along each vertical axis is core depth in feet. LST = lowstand systems tract, TST = transgressive systems tract, HST = highstand systems trace, SB = sequence boundary.

and sand content increases. Lithology changes from muddy carbonate (TST) to calcareous sand (HST).

In the younger highstand sediments, lithified zones decrease in thickness and frequency. Mottling becomes less frequent and more indistinct. Faunal assemblages shift from dominantly foraminiferal in the TST to mollusk, crinoid and echinoid fragment dominant in HST. The upper part of the highstand is characterized by thin clay laminations and thin lithified zones (less than 0.5 ft. thick) separated by sand. Table 2 summarizes these characteristics.

Lithified horizons within the highstand are interpreted as marine hardgrounds. In the early highstand sediments these surfaces are relatively thick and highly bioturbated, due either to the greater availability of accommodation on the shelf or to low sedimentation rates. Later in the highstand these zones decrease in thickness and are not as highly burrowed, reflecting a decrease in accommodation and sedimentation rates as highstand conditions persist (Emery and Myers, 1996).

The boundary between Sequence 2 and Sequence 3 occurs at a depth of 318 ft. and is more subtle than the previously described sequence boundary. Lithologically, it is marked by a final lithified horizon that is much finer grained than the top of the underlying HST. A clay lamination is in sharp contact with the lithified horizon, which has a glauconite content of approximately 20%. Crinoid columnals are no longer present and no shells are visible in this section of the core.

Sequence Boundary 2 (SB-2) is interpreted as a Type-2 sequence boundary. The minor shift in facies and mineralogy suggests a slow relative fall of sea level. Fraser (1989) suggests that sequence boundaries may be marked by relict surfaces as well as authigenic minerals such as

Table 2: Characteristics of Sequence 2, Kure Beach core.

Kure Beach Core Description	**Sequence 2 LSW**	**Sequence 2 TST**	**Sequence 2 HST**
Depth (ft.)	410-399	399-374	374-318
Color	olive-gray	olive-gray	olive-gray
Lithology	muddy carbonate	muddy carbonate	sandy carbonate/calcareous sand
Bedding	massive/bioturbated	bioturbated	bioturbated
Induration	friable	lithified/friable	lithified/friable
Quartz	VA-D	VA-D	D
Glauconite	R-A	R	
Phosphate	T	T-R	T-R
Mica	T-R	R	T-R
Crinoids	-	R	R-C
Mollusks	T	R	R
Benthic Foraminifera	R	R	R
Planktonic Foraminifera	T	R	R
Age	Maastrichtian	Maastrichtian	Maastrichtian
Sedimentological Characteristics of Sampled Population			
Carbonate (mean wt. %)	33.1	65.2	36.7
Terrigenous Fraction (mean wt. %)			
Percent Gravel	0	0	0
Percent Sand	49.5	11.5	41.2
Percent Mud	22.3	23.6	13.8
Mean grain size (φ)	2.47 (upper fine sand)	2.92 (lower fine sand)	2.63 (lower fine sand)
Sorting (φ)	0.91 (moderately sorted)	0.98 (moderately sorted)	0.70 (moderately well-sorted)
Skewness	-0.05 (near symmetrical)	0.15 (fine-skewed)	-0.39 (strongly coarse-skewed)
Kurtosis	2.46 (very leptokurtic)	0.66 (very platykurtic)	3.35 (extremely leptokurtic)
Roundness	subangular/subrounded	subangular	subangular/subrounded

Index: D = Dominant (>75%) VA = Very Abundant (51-75%) A = Abundant (26-50%)
C = Common (15-25%) R = Rare (1-15%) T = Trace (<1%) - = Not observed

glauconite and phosphate. Relatively large amounts of both glauconite and phosphate are present above the sequence boundary and the final lithified horizon may represent a relict surface. No evidence of subaerial exposure is present and there are no pebble zones or lags to suggest a major ravinement surface. Sorting becomes poorer above SB-2 and carbonate content decreases slightly (~ 5%). The interval from 320 ft. to 318 ft. was lost during drilling and may contain the unconformity separating S-1 from S-2. Also, the placement of the boundary will most likely be constrained further once biostratigraphic or strontium isotope data becomes available.

Sequence 3

Sequence 3 (318 ft. – 152 ft.) is interpreted to contain a thin shelf margin wedge (SMW), a thin transgressive deposit (TST) and a thicker highstand deposit (HST) that can be separated into early and late parts (Fig. 17). The SMW (318 ft. – 300 ft.) is characterized by lower fine sand and shows a slight increase in sand percentage up-section, suggesting a progradational geometry. Carbonate content is between 30% and 45% and decreases upward. Above 300 ft., carbonate and clay percentages sharply increase, marking the surface of maximum progradation (Emery and Myers, 1996). The gamma ray log also changes from a lower progradational to an upper retrogradational/aggradational geometry (Fig. 18). This change in geometry marks the beginning of the transgressive systems tract (300 ft. – 263 ft.). Mud content and relative abundance of planktonic Foraminifera greatly increase at this point, signaling a rapid transition to deeper water deposits and the beginning of the condensed section, which may extend to 258 ft.

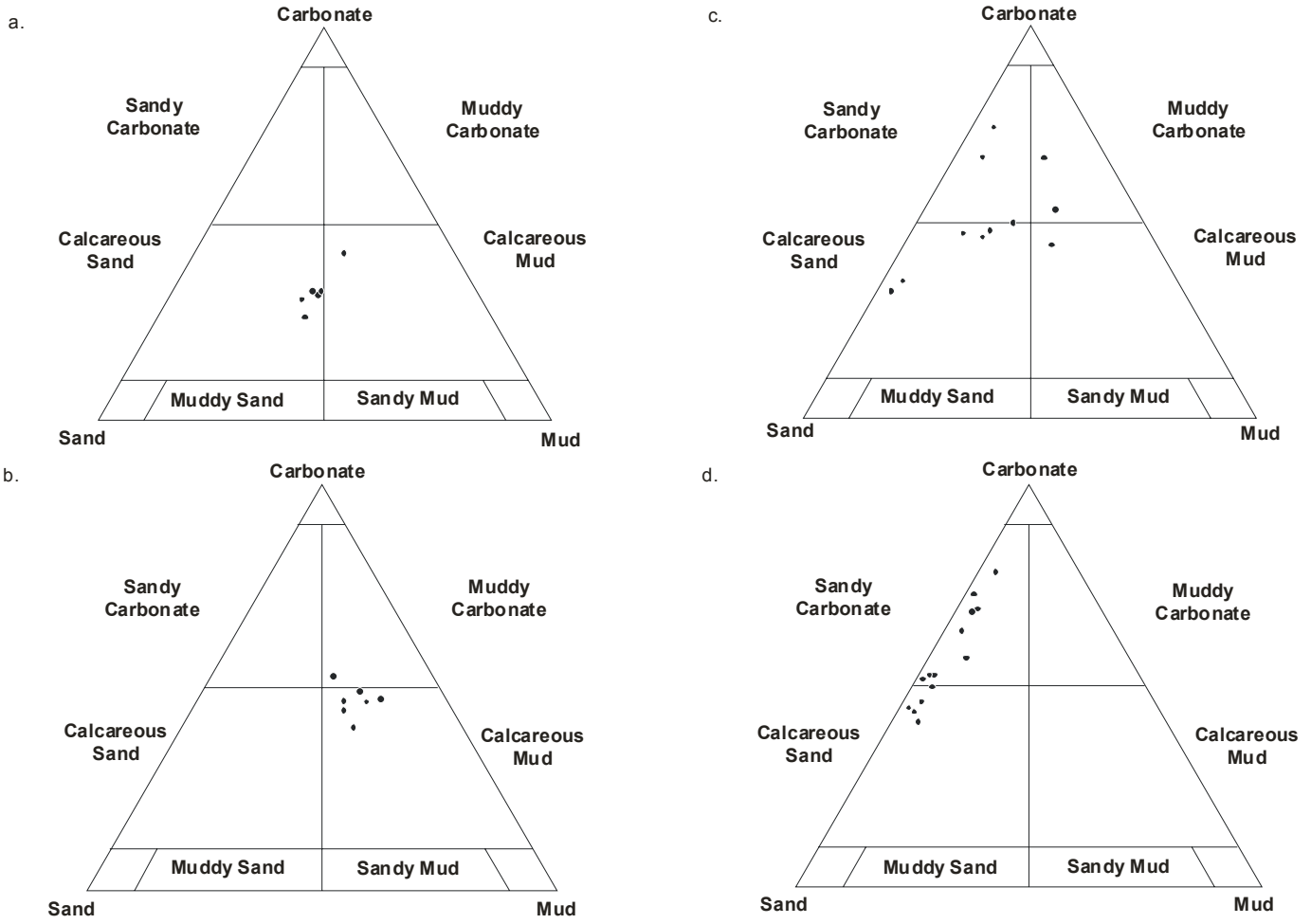

Figure 17. Lithologic comparison between systems tracts in Sequence 3 (a) shelf margin deposits (SMST), (b) transgressive deposits (TST), (c) early and (d) late highstand deposits (HST), Kure Beach core. Fields after Lindholm (1987).

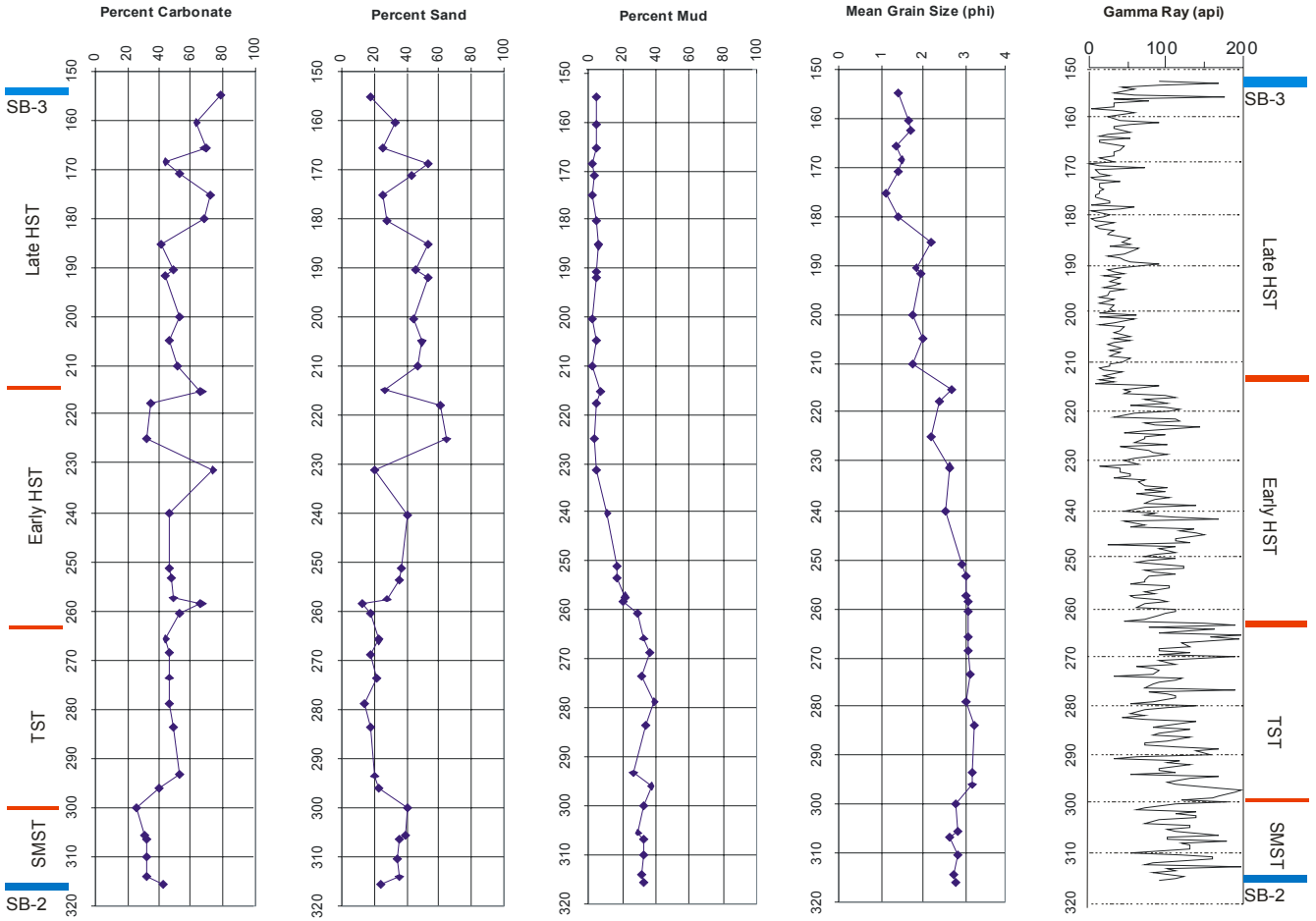

Figure 18. Graphical representation of Sequence 3 lithology in the Kure Beach core. Along each vertical axis is core depth in feet. SMST = shelf margin systems tract, TST = transgressive systems tract, HST = highstand systems tract, SB = sequence boundary.

Stacking geometry becomes more aggradational upcore from the SMF (Fig. 18) in the early highstand. The overlying highstand deposit (263 ft. – 152 ft.) is characterized by two sediment packages representing early and late highstand. The early highstand (263 ft. – 215 ft.) maintains an aggradational geometry, only prograding slightly beyond the TST. Grain size coarsens upward. Quartz is the dominant mineral in all samples, above 90% in most.

At 250 ft, lithified areas begin again, but are not always horizontal bands. Instead, they are generally small (1-2 in.) and rounded. They at first appear to be intraclasts, but are not of similar lithology to the underlying lithified areas. It is more likely that the lithified areas are concretions and represent areas of in-situ dissolution of shell material and aggrading neomorphism of the calcite matrix.

The early highstand is divided from the late highstand by a parasequence boundary marked by finer grain sizes and a change in carbonate content that is interpreted to signal a marine flooding event. Above the boundary, in the late highstand (215 ft. – 152 ft.), carbonate increases and lithified clasts are present in the upper part. These lithified materials are not highly cemented and contain abundant shell fragments—bivalves, bryozoans, gastropods and ostracodes are most commonly identified. In the late highstand sediments there is also evidence of shoaling and winnowing of materials. The sample at 210 ft., at the base of the youngest highstand, contains large quartz grains and highly bored shell fragments. Wave effects are evidenced by fragmented benthic Foraminifera, but the presence of micrite suggests that deposition was still below normal wave base. Still higher lithified clasts show more borings and void space, with blocky calcite cement. Mollusks increase and Foraminifera decrease. Sediments become cleaner and coarser upsection. Allochems in the youngest highstand sediments contain micrite envelopes. A dense coating of micrite is present in the uppermost sample, suggesting proximity

to an unconformity. A comparison between sediment types interpreted to represent the various systems tracts of Sequence 3 are shown in Table 3.

Sequence 4

Sequence 4 (152 ft. to 130 ft) is interpreted to range from latest Maastrichtian to Paleocene. Thus, the upper extent of Sequence 4 is not included in this study. The base of the sequence is characterized by a nearly pure carbonate overlain by relatively clean muddy sand. Above the muddy sand lies very dark calcareous mud. The increase in mud content around 137 ft is thought to represent late Maastrichtian sediments grading across the K-T boundary into the Danian (Fig. 19). Baum (1986) demonstrated that sediments from South Carolina also spanned this time period. In the Kure Beach core this surface is interpreted to represent a surface of maximum flooding (MFS). A summary of Sequence 4 sediment characteristics can be found in Table 4.

Hilton Park Core

Sequence 1

Sequence 1 (62 ft. – 47 ft.) is interpreted to represent a highstand deposit (Figure 19). The section is characterized by alternating sandy pelecypod mold grainstone and sandy carbonate intervals. Carbonate content is relatively high (48%) and mud content is low, averaging about 10% (Fig.21). Benthic Foraminifera are common; planktonic Foraminifera were not observed. These data suggest Sequence 1 is a late highstand deposit, similar to late highstand sediments in the Kure Beach core. An indurated horizon below 41 ft. is interpreted to represent an unconformity and the boundary between Sequences 1 and 2.

Table 3. Characteristics of Sequence 3, Kure Beach core.

Kure Beach Core Description	**Sequence 3 SMST**	**Sequence 3 TST**	**Sequence 3 early HST**	**Sequence 3 late HST**
Depth (ft.)	318-300	300-263	263-215	215-152
Color	olive-gray	olive-gray	olive-gray	olive-gray/dusky yellow
Lithology	calcareous sand/calcareous mud	muddy carbonate	muddy/sandy carbonate	calcareous sand
Bedding	bioturbated	clay laminations	bioturbated	bioturbated
Induration	friable/lithified	friable/concretions	friable/concretions	friable/concretions
Quartz	VA	VA-D	VA-D	D
Glauconite	R-C	R	T-R	T
Phosphate	R	R	T-R	T-R
Mica	R	R	T-R	T
Crinoids	-	-	-	-
Mollusks	R	R	R	R-C
Benthic Foraminifera	R	R	R-C	R
Planktonic Foraminifera	T	T	R	T
Age	Maastrichtian	Maastrichtian	Maastrichtian	Maastrichtian
Sedimentological Characteristics of Sampled Population				
Carbonate (mean wt. %)	32.8	47.4	51.8	56.7
Terrigenous Fraction (mean wt. %)				
Percent Gravel	0	0	0	0
Percent Sand	35.2	19.6	37.7	39.2
Percent Mud	32.0	35.6	10.6	4.05
Mean grain size (φ)	2.78 (lower fine sand)	3.12 (lower very fine sand)	2.64 (lower fine sand)	1.64 (lower medium sand)
Sorting (φ)	0.81(moderately sorted)	0.57 (moderately well-sorted)	0.55 (moderately sorted)	0.69 (mod. well-sorted)
Skewness	-0.54 (strongly coarse-skewed)	-0.41 (strongly coarse-skewed)	0.06 (near symmetrical)	-0.01 (near symmetrical)
Kurtosis	3.52 (extremely leptokurtic)	1.5 (leptokurtic)	2.31 (very leptokurtic)	2.27 (very leptokurtic)
Roundness	subangular	subangular	subrounded/rounded	subangular/subrounded

Index: D = Dominant (>75%) VA = Very Abundant (51-75%) A = Abundant (26-50%)
C = Common (15-25%) R = Rare (1-15%) T = Trace (<1%) - = Not observed

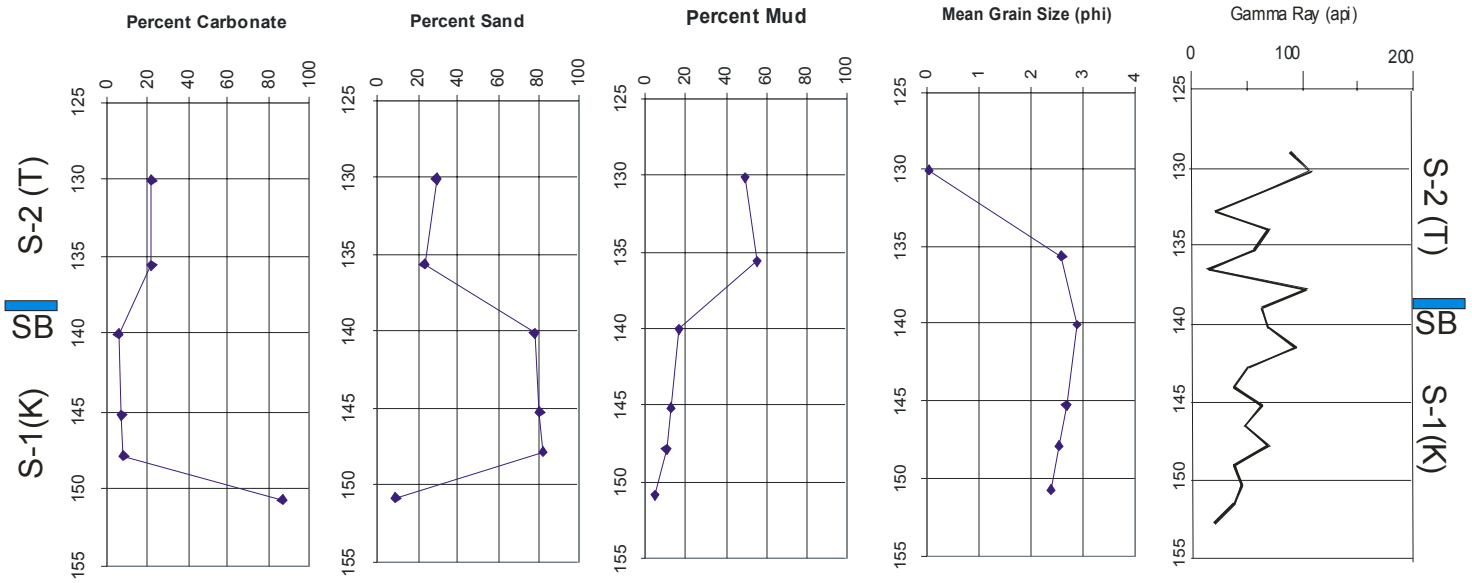

Figure 19. Graphical representation of Sequence 4 lithology in the Kure Beach core. Along each vertical axis is core depth in feet. S-1 = sequence 1, S-2 = sequence 2, SB = sequence boundary, K = Cretaceous, T = Tertiary.

Table 4. Charcteristics of Sequence 4, Kure Beach core

Kure Beach	
Core Description	**Sequence 4**
Depth (ft.)	152-130
Color	olive-gray/olive-black
Lithology	carbonate/sand/calcareous mud
Bedding	bioturbated
Induration	unconsolidated/concretions
Quartz	D-VA
Glauconite	T-C
Phosphate	T-R
Mica	T-R
Crinoids	-
Mollusks	T-R
Benthic Foraminifera	T-R
Planktonic Foraminifera	-
Age	Maastrichtian (?) to Danian (?)

Sedimentological Characteristics of Sampled Population

Carbonate (mean wt. %)	25.1
Terrigenous Fraction (mean wt. %)	
Percent Gravel	0
Percent Sand	50.2
Percent Mud	24.7
Mean grain size (φ)	2.19 (upper fine sand)
Sorting (φ)	1.02 (poorly sorted)
Skewness	0.23 (fine-skewed)
Kurtosis	2.09 (very leptokurtic)
Roundness	subangular/subrounded

Index: D = Dominant (>75%) VA = Very Abundant (51-75%) A = Abundant (26-50%)
C = Common (15-25%) R = Rare (1-15%) T = Trace (<1%) - = Not observed

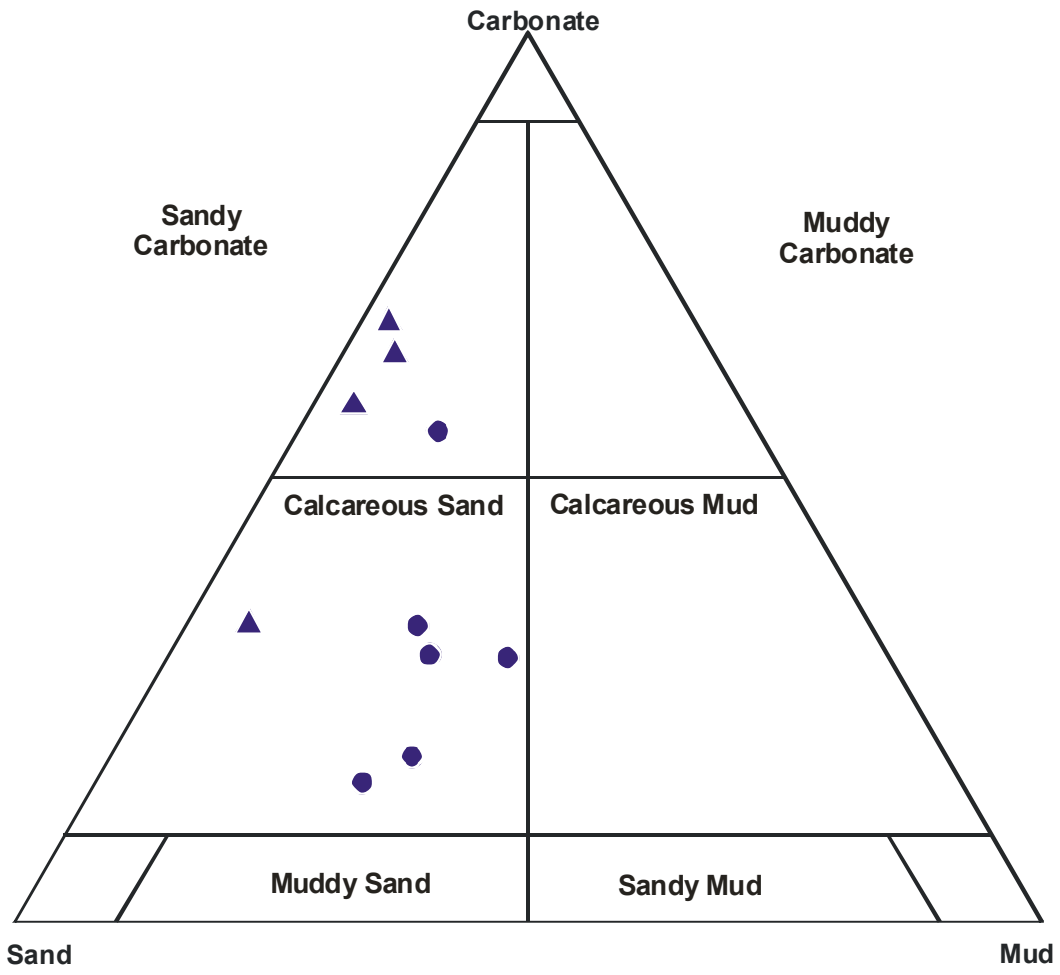

Figure 20. Lithologic comparison between Sequence 1 (triangles) and Sequence 2 (circles), Hilton Park core. Fields after Lindholm (1987).

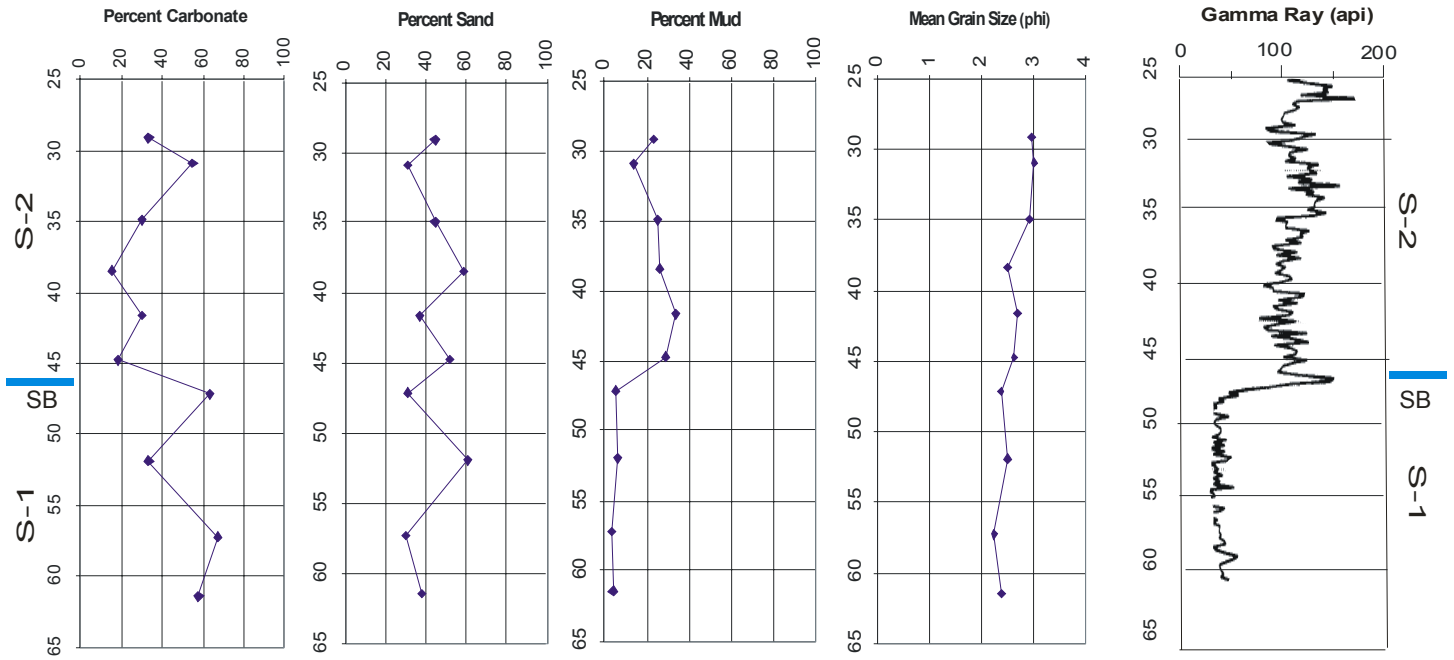

Figure 21. Graphical representation of Sequence 1 and 2 lithology in the Hilton Park core. Along each vertical axis is core depth in feet. S-1 = sequence 1, S-2 = sequence 2, SB = sequence boundary.

Table 5. Characteristics of Sequences 1 and 2, Hilton Park core.

Hilton Park Core Description	**Sequence 1**	**Sequence 2**
Depth (ft.)	62-47	47-26
Color	light olive gray/ olive gray	dark greenish gray
Lithology	grainstone/ sandy carbonate	sandy carbonate/calcareous sand
Bedding	massive	massive
Induration	lithified/unconsolidated	unconsolidated
Quartz	D	D
Glauconite	T-R	R
Phosphate	T-R	R
Mica	T-R	R
Crinoids	-	-
Mollusks	R	T-R
Benthic Foraminifera	R	T-R
Planktonic Foraminifera	-	-
Age	Maastrichtian	Maastrichtian/ Danian (?)
Sedimentological Characteristics of Sampled Population		
Carbonate (wt. %)	48.22	32.87
Terrigenous Fraction (wt. %)		
Percent Gravel	0	0
Percent Sand	42.27	42.95
Percent Mud	9.51	24.18
Mean grain size (φ)	2.42 (upper fine sand)	2.81 (lower fine sand)
Sorting (φ)	0.52 (moderately well-sorted)	0.65 (moderately well-sorted)
Skewness	-0.16 (coarse-skewed)	-0.13 (coarse-skewed)
Kurtosis	4.52 (extremely leptokurtic)	2.41 (very leptokurtic)
Roundness	subangular/subrounded	subangular

Index: D = Dominant (>75%) VA = Very Abundant (51-75%) A = Abundant (26-50%)
C = Common (15-25%) R = Rare (1-15%) T = Trace (<1%) - = Not observed

Sequence 2

Sequence 2 (47 ft. – 26 ft.) is interpreted to represent a transgressive deposit (TD), characterized by a significant increase in mud content (9.51% to 24.18%) above the unconformity at 47 ft. (Fig. 21) The sediments above the unconformity are poorly indurated, have a higher authigenic mineral content and are darker in color. Mollusks and benthic Foraminifera are still present, but in small amounts. Planktonic Foraminifera were not identified. These data suggest a slight deepening of water between Sequences 1 and 2. A summary of these sequences is found in Table 5.

Black Rock Landing

Sequence 1

Sequence 1 (54 ft. – 41 ft.) is interpreted to represent a highstand deposit (HD) (Fig. 22). The greenish black, medium-grained calcareous sand contains mollusk fragments that are often concentrated in one area and commonly occur as concretionary masses. The authigenic mineral content of the sediments is relatively high. Benthic Foraminifera are present, but no planktonic Foraminifera were observed. An unconformity is visible at 43 ft. and corresponds to a large lag deposit in exposures on the Cape Fear River at Black Rock Landing. This unconformity is interpreted to represent a sequence boundary.

Sequence 2

Sequence 2 (41 ft. – 29 ft.) is interpreted to represent a transgressive deposit (TD). Mean grain size fines abruptly across the unconformity, from 1.7 φ in Sequence 1 to 3.3 φ in Sequence 2 (Fig. 22). The sediments are slightly darker in color, are better sorted, and have a slightly lower authigenic mineral content (Table 6). Mollusk fragments are less common and benthic Foraminifera are present in all samples. Planktonic foraminifera were not observed.

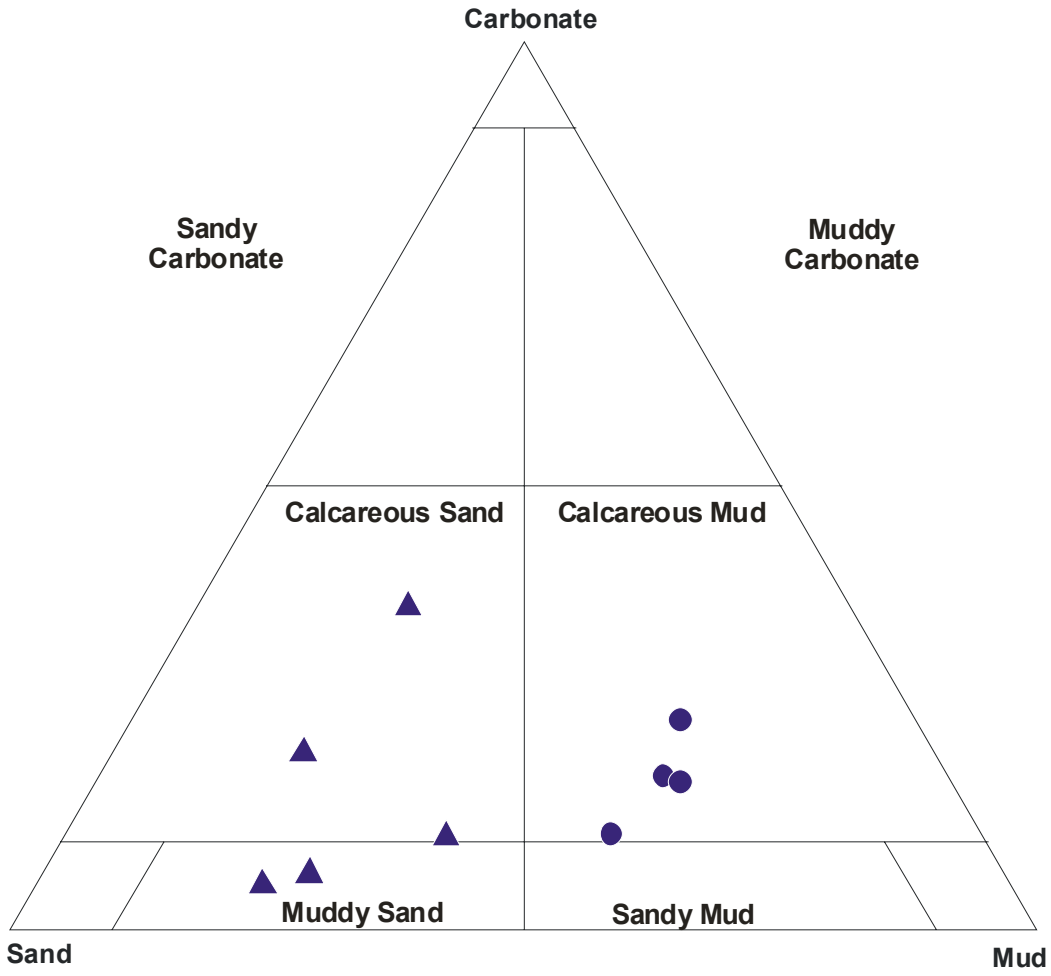

Figure 22. Lithologic comparison between Sequence 1 (triangles) and Sequence 2 (circles), Black Rock Landing core. Fields after Lindholm (1987).

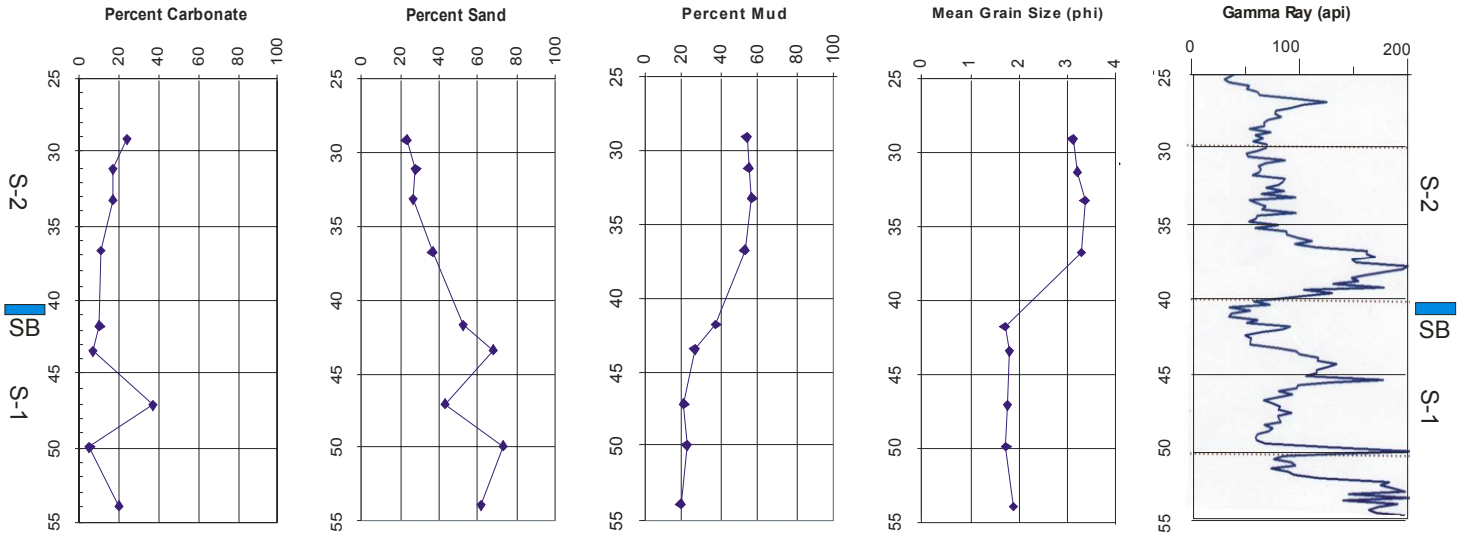

Figure 23. Graphical representation of Sequences 1 and 2 lithology in the Black Rock Landing core. Along each vertical axis is core depth in feet. S-1 = sequence 1, S-2 = sequence 2, SB = sequence boundary.

Table 6. Characteristics of Sequences 1 and 2, Black Rock Landing core.

Black Rock Landing Core Description	**Sequence 1**	**Sequence 2**
Depth	54-41	41-25
Color	greenish black/olive black	greenish black
Lithology	calcareous sand	calcareous mud
Bedding	massive/bioturbated	massive/bioturbated
Induration	friable/concretions	unconsolidated
Quartz	D	VA
Glauconite	T-R	R
Phosphate	T-R	R
Mica	R	R
Crinoids	-	-
Mollusks	R	T
Benthic Foraminifera	R	R
Planktonic Foraminifera	-	-
Age	Campanian	Maastrichtian
Sedimentological Characteristics of Sampled Population		
Carbonate (mean wt. %)	15.6	17.1
Terrigenous Fraction (mean wt. %)		
Percent Gravel	0	0
Percent Sand	59.5	28.3
Percent Mud	24.9	54.6
Mean grain size (φ)	1.78 (lower medium sand)	3.24 (upper very fine sand)
Sorting (φ)	0.93 (moderately sorted)	0.52 (moderately well-sorted)
Skewness	-0.07 (near symmetrical)	-0.48 (strongly coarse-skewed)
Kurtosis	2.52 (very leptokurtic)	2.80 (extremely leptokurtic)
Roundness	subangular	subangular

Index: D = Dominant (>75%) VA = Very Abundant (51-75%) A = Abundant (26-50%)
C = Common (15-25%) R = Rare (1-15%) T = Trace (<1%) - = Not observed

CORRELATION

Sequence 1

Sequence 1 in the Kure Beach core (467 ft. – 410 ft.) and Sequence 1 in the Black Rock Landing core (54 ft. – 43 ft.) are interpreted to represent the same depositional sequence based on lithology and biostratigraphic data (Fig 24). This sequence is exposed from Donoho Creek Landing (mile 50.2) to just below Lock and Dam #1 at Kings Bluff (mile 38) on the Cape Fear River. It may be exposed at extreme low water at Black Rock Landing (mile 37) based on bluff elevation and depth identified to the top of the sequence in the Black Rock Landing core. Sequence 1 corresponds to the Donoho Creek Formation of Sohl and Owens (1991). Paleontologic data from Self Trail et al. (2002) indicate that the Donoho Creek sequence is late Campanian in age and is correlated to calcareous nannofossil zones CC22a and CC23.

Sequence 2

Sequence 2 in the Kure Beach core (410 ft. – 318 ft.) and Sequence 2 in the Black Rock Landing core (43 ft. – 29 ft.) are interpreted to represent the same depositional sequence based on lithology and biostratigraphic data (Fig. 24). This sequence is exposed from Black Rock Landing (mile 37) to Wanets Landing (milepost 25) on the Cape Fear River. Sequence 2 corresponds the late Maastrichtian Peedee Formation (Stephenson, 1912, 1923). Biostratigraphic data taken from Sequence 2 in the Kure Beach core indicates a Maastrichtian age for the sequence and a correlation to calcareous nannofossil zone 25 b.

The boundary between Sequences 2 and 3 is interpreted to correspond to the 71 Ma sequence boundary described on the Exxon global cycle chart (Haq et. al, 1987). This boundary is not seen on the Cape Fear River in outcrop, but may occur between Wanets Landing (milepost 25) and Strawberry Hill Landing (milepost 18.2). The cyclicity of hardgrounds and clay-rich

layers of Kure Beach Sequence 2 late highstand is evidenced at Wanets Landing (mile 25), and large displaced chunks of the Rock Point Member were found near Strawberry Hill (mile 18.2). The boundary is therefore predicted to occur on the Cape Fear River near mile 22.

Sequence 3

Sequence 3 in the Kure Beach core (318 ft. – 152 ft.) and Sequence 1 in the Hilton Park core (62 ft. – 47 ft.) are interpreted to represent the same depositional sequence based on lithologic similarity (Fig. 24). Sequence 3 corresponds to the late Maastrichtian Rocky Point Member of the Peedee Formation (Harris, 1978).

The dissolution surface at the top of Kure Beach Sequence 3 late highstand sediments was first interpreted as the Cretaceous-Tertiary boundary, but is now thought to represent the 68 Ma sequence boundary of the Exxon cycle chart (Haq, et.al, 1987). This unconformity is more subtle in the Hilton Park core, but is thought to be represented by an unconformity at 47 ft.

Sequence 4

Sequence 4 in the Kure Beach core (152 ft. – 137 ft.) and Sequence 2 in the Hilton Park core are interpreted to represent the same depositional sequence based on lithology and biostratigraphic data (Fig. 24). Sequence 4 is exposed at Hilton Park (mile 0) on the Cape Fear River. A thin-section taken above the boundary contains dolomite rhombs (Fig. 8c). This evidence, coupled with similar color and lithology, enables correlation of Sequence 4 to the Island Creek Member of the Peedee Formation. Biostratigraphic data taken from the Island Creek Member indicates a late Maastrichtian age for the sediments and is correlated to calcareous nannofossil zones CC 25 – CC 26 (Dockal et. al, 1998).

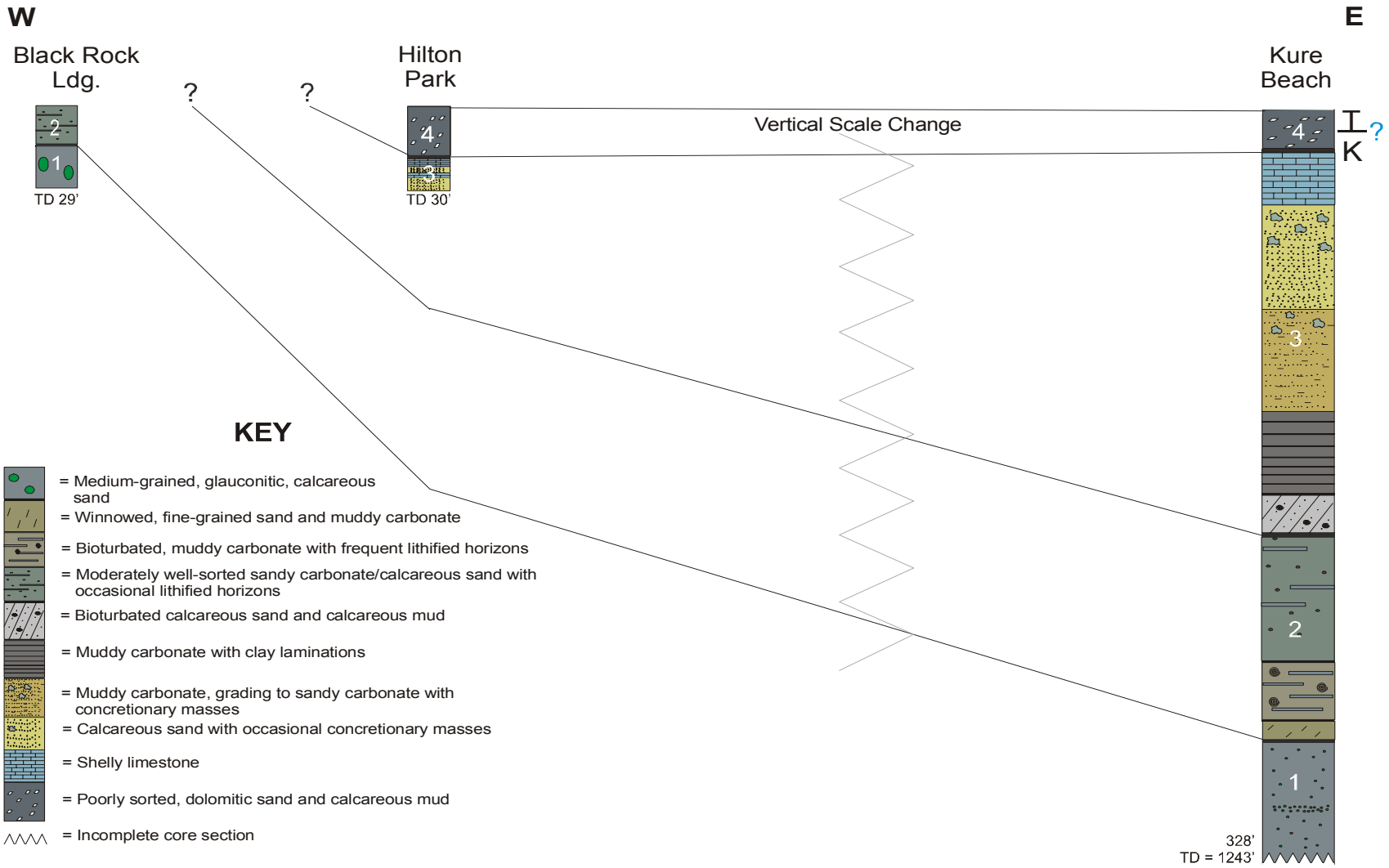

Figure 24. Summary cross section of Cretaceous units in study area. The numbers refer to the correlated sequences.

CONCLUSIONS

The following conclusions can be made from the data obtained from all three cores and combined with information obtained from outcrop observations:

1. Four depositional sequences are present in the Kure Beach core.
2. Sequence 1 is characterized by medium-grained, olive gray, glauconitic calcareous sand. It is interpreted to consist of two parasequences within a highstand deposit, the lower part of which was not studied. This sequence is correlated to the late Campanian Donoho Creek Formation of the Black Creek Group.
3. Sequence 1 is separated from Sequence 2 by a Type-1 sequence boundary at 410 ft. The presence of this boundary is supported lithologically by an unconformable surface and biostratigraphically by the absence of calcareous nannofossil zones CC24 and CC25a.
4. Sequence 2 begins with a winnowed, fine-grained, olive-gray muddy carbonate. A lithified horizon separates the basal lithology from midsection bioturbated, olive-gray muddy carbonate. Lithified horizons begin to increase in frequency and are often highly bioturbated. The upper part of the sequence is characterized by olive-gray sandy carbonate and calcareous sand with fewer lithified horizons. Sequence 2 contains a sandy, winnowed lowstand wedge overlain by a transgressive surface. A thin transgressive deposit overlies the transgressive surface and is followed by a thicker highstand systems tract. The HST is characterized by burrowed, lithified horizons that become less frequent upcore. This sequence is correlative to basal Peedee Formation and is Maastrichtian in age.
5. A Type-2 sequence boundary separates Sequences 2 and 3 at 318 ft. The unconformity that represents this boundary is more indistinct than the unconformity at the previous sequence boundary and contains reworked materials derived from Sequence 2. Further

biostratigraphic data are needed to constrain the exact boundary position. Up-dip the boundary is thought to occur along the Cape Fear River in the area between Wanets Landing and Strawberry Hill Landing, near milepost 22, but it is covered by more recent sediments.

6. Sequence 3 consists of a basal, olive-gray, bioturbated calcareous sand. The basal sand is overlain by a muddy carbonate with clay laminations. Higher in the sequence the muddy carbonate grades into a dusky yellow sandy carbonate and calcareous sand. Concretionary masses are present in these sediments and increase in frequency upsection. The top of the sequence is characterized by a sandy pelecypod-mold grainstone. Sequence 3 is interpreted to contain a shelf margin deposit followed by a transgressive systems tract. Sediments in the TST are muddy and contain abundant benthic and planktonic Foraminifera, suggesting deeper water conditions. A highstand systems tract overlies the TST and is characterized by early and late parts separated by a flooding surface. The contact is sharp and marked by finer-grained sediments. The early highstand is aggradational/progradational whereas late highstand is progradational. Both early and late parts coarsen upward. The late highstand corresponds to the late Maastrichtian Rocky Point Member of the Peedee Formation and is capped by the 68 Ma Type-1 Sequence boundary of the Exxon global cycle chart.
7. A sequence boundary separates Sequences 3 and 4 at 152 ft. The unconformity is marked by a very hard, light gray nearly pure carbonate. It represents the 68 Ma Type-1 Sequence Boundary of the Exxon global cycle chart.
8. Sequence 4 is characterized by basal olive gray dolomitic calcareous sand and upper olive black calcareous mud. This sequence is correlative to the late Maastrichtian Island Creek Member of the Peedee Formation that grades upward into Danian (?) age sediments. The K/T boundary is thought to occur somewhere around 138 ft.

9. The Hilton Park core consists of basal, light olive gray calcareous sand alternating with light olive gray sandy pelecypod mold grainstone. An indurated zone separates these lithologies from upper dark gray dolomitic sandy carbonate and calcareous sand. The Hilton Park core correlates to Kure Beach Sequence 3 late highstand, which shoals up to typical Rocky Point lithology. Also present in the Hilton Park core are sediments of typical Island Creek lithology. These sediments correspond to latest Maastrichtian sediments found in Sequence 4 of the Kure Beach core.
10. The Black Rock Landing core consists of a basal, olive black calcareous sand. An unconformity around 43 ft. separates the basal lithology from upper greenish black calcareous mud. The Black Rock Landing core is correlative to the uppermost highstand of Sequence 1. The boundary found around 43 ft. may represent the first sequence boundary. The large shelf lag located on the Cape Fear River at river level may correspond to the indurated transgressive surface found above Sequence Boundary 1 in the Kure Beach core.

REFERENCES CITED

Balsille, J.H., Donoghue, J.F., Butler, K.M., and Koch, J.L., 2002, Plotting equation for Gaussian percentiles and a spreadsheet program for generating probability plots: Journal of Sedimentary Research, v. 27, p. 929-943

Baum, G.R., 1986, Sequence stratigraphic concepts as applied to the Eocene carbonates of the Carolinas, in D. A. Textoris, ed., SEPM Guidebooks Southeastern United States, Third Annual Midyear Meeting, Raleigh, North Carolina: Society of Economic. Paleontologists and Mineralogists, p.264-269.

Custer, E. S., 1981, Depositional environments of the subsurface Cretaceous deposits of southeastern North Carolina: PhD. Dissertation, University of North Carolina, Chapel Hill, 116 p.

Dockal, J.A., Harris, W.B., and Laws, R. A., 1998, Late Maastrichtian sediments on the north flank of the Cape Fear Arch: Southeastern Geology, v. 37, p. 149-159.

Emery, D. and Myers, K., 1996, Sequence Stratigraphy: Oxford, Blackwell Science, 297 p.

Farrell, K.M., 1998, The Cretaceous Cape Fear and Black Creek Formations of Southeastern North Carolina: Cape Fear River traverse—milepost 110 to milepost 60, in Field Trip Guidebook, Carolina Geological Survey Annual Meeting: Durham, Duke University Press in association with the North Carolina Geological Survey.

Farrell, K.M., Ward, L.W., and Heron, S.D., Jr., 2001, Cape Fear River transect: The Upper Cretaceous Cape Fear, Black Creek, and Peedee Formations of Southeastern North Carolina and the overlying Cenozoic section (MP 111 to MP 25), in Field Trip

Guidebook, 50th Annual Meeting, Southeastern Section, Geological Society of America, Raleigh, North Carolina, p. 93-118.

Finneran, J.M., 1980, Calcareous nannofossil biostratigraphy and structure of Upper Cretaceous sediments of the North Carolina coastal plain: Masters Thesis, Ohio University, Athens, 116 p.

Folk, R.L. and Ward, W.C., 1957, Brazos River bar: a study in the significance of grain size parameters: Journal of Sedimentary Petrology, v. 27, p. 3-26.

Fraser, G.S., 1989, Clastic depositional sequences: processes of evolution and principles of interpretation: Englewood Cliffs, Prentice Hall, 459 p.

Haq, B.U., Hardenbol, J., and Vail, P.R., 1987, Chronology of fluctuating sea levels since the Triassic: Science, 235, p. 1156-1166.

Harris, W.B., 1978, Stratigraphic and structural framework of the Rocky Point Member of the Cretaceous Peedee Formation: Southeastern Geology, v. 19, p. 207-229.

Heron, S.D., Jr., 1958, The stratigraphy of the outcropping basal Cretaceous formations between the Neuse River, North Carolina, and Lynches River, South Carolina: PhD. Dissertation, University of North Carolina, Chapel Hill, 155 p.

Heron, S.D., Jr., and Wheeler, W. H., 1964, The Cretaceous formations along the Cape Fear River, North Carolina: Atlantic Coastal Plain Geological Association Field Guide, Fifth Annual Field Excursion, Oct. 1964, 55 p.

Ireland, H.A., 1977, Insoluble residues; in LeRoy, L.W., LeRoy, D.O., and J.W. Raese, eds. Subsurface geologic methods, 4th edition: Golden, Colorado, Colorado School of Mines, p. 53-60.

Lindholm, R.C., 1987, A practical approach to sedimentology: London, Allen & Unwin, 276 p.

Miall, A. D., 1997, The Geology of Stratigraphic Sequences. Berlin: Springer-Vorlag, 433 p.

Mitchum, R.M., Jr., Vail, P.R., and Sangree, J.B., 1977, Seismic stratigraphy and global changes of sea level, Part 2, the depositional sequence as a basic unit for stratigraphic analysis, in Payton, C.E., ed. Seismic Stratigraphy—Applications to Hydrocarbon Exploration. AAPG Memoir 26, p. 53-62.

Mitchum, R.M., Jr., Sangree, J.B., Vail, P.R., and Wornardt, W.W., 1994, Recognizing sequences and systems tracts from well logs, seismic data, and biostratigraphy: examples from the late Cenozoic, p. 163-198.

Nummedal, D. and Swift D. J.P., 1987, Transgressive stratigraphy at sequence-bounding unconformities: some principles derived from Holocene and Cretaceous examples; in Nummedal, D., Pilkey, O.H, and Howard, J.D., eds. Sea Level Fluctuation and Coastal Evolution: SEPM Special Publication No. 41, p. 241-260.

Owens, J.P., 1989, Geologic Map of the Cape Fear Region, Florence 1° x 2° Quadrangle and northern half of the Georgetown 1° x 2° Quadrangle, North and South Carolina: U.S. Geological Survey, Miscellaneous Investigations Series, map I-1948-A.

Posamentier, H.W. and Vail, P.R., 1988, Eustatic controls on clastic deposition II—sequence and systems tract models. in Wilgus, C.K., Hastings, B.S., Kendall, C. C. St. C, Posamentier, H.W., Ross, C.A., and Van Wagoner, J.C., eds. Sea Level Changes—an Integrated Approach: SEPM Special Publication No. 42, p.125-154.

Prowell, D.C., Christopher, R.A., Waters, K.E., and Nix, S.K., 2003, The chrono- and lithostratigraphic significance of the type section of the Middendorf Formation, Chesterfield County, South Carolina: Southeastern Geology, v. 42, no. 1, p. 47-66.

Self-Trail, J.M., 2001, Biostratigraphic subdivision and correlation of Upper Maastrichtian sediments from the Atlantic Coastal Plain and Blake Nose, Western Atlantic. in Kroon, D., Norris, R.D., and Klaus, A., eds. Western North Atlantic Palaeogene and Cretaceous Palaeooceanography: London, Geological Society Special Publications 183, p. 93-110.

Self-Trail, J.M., Christopher, R.A. and Prowell, D.C., 2002, Evidence for large-scale reworking of Campanian sediments into the upper Maastrichtian Peedee Formation at Burches Ferry, South Carolina: Southeastern Geology, v. 41, no. 3, p.145-158

Sohl, N.F. and Owens, J.P., 1991, Cretaceous stratigraphy of the Carolina Coastal Plain. in Horton, J.W., Jr. and Zullo, V.A. eds. The Geology of the Carolinas: Knoxville, University of Tennessee Press, p. 191-220.

Stephenson, L.W., 1912, The Cretaceous Formations. in Clark, W.B., Miller, B.L., Stephenson, L.W., Johnson B.L. and Parker, H.N., The Coastal Plain of North Carolina. North Carolina Geologic and Economic Survey, v.3, p. 73-171.

Stephenson, L.W., 1923, Invertebrate fossils of the Upper Cretaceous Formations of North Carolina: North Carolina Geologic and Economic Survey, v. 5, Part I, 604 p.

Swift, D. J. P., 1964, Origin of the Cretaceous Peedee Formation of the Carolina Coastal Plain: PhD Dissertation, University of North Carolina, Chapel Hill, 151 p.

Swift, D.J.P. and Heron, S.D., Jr., 1969, Stratigraphy of the Carolina Cretaceous: Southeastern Geology, v. 10, p. 201-245.

The Rock Color Chart Committee, 1975, Rock Color Chart, Huyskes-Enschede, the Netherlands, distributed by the Geological Society of America, New York, 11 p.

Vail, P.R., Mitchum, R.M., Jr., Todd, R.G., Widmier, J.M., Thompson S III, Sangree,

J.B, Bubb, J.N., and Hatleid, W.G., 1977, Seismic stratigraphy and global changes in sea level; in Payton, C., ed. Seismic Stratigraphy—applications to hydrocarbon exploration. AAPG Memoir 26:49-212.

Van Wagoner, J.C., Posamentier, H. W., Mitchum, R.M., Vail, P.R., Sarg, J.F., Loutit, T.S., and Hardenbol, J., 1988, An overview of the fundamentals of sequence stratigraphy and key definitions, in Wilgus, C.K., Hastings, B.S., Kendall, C.G. St. C., Posamentier, H.W., Ross, C.A. and Van Wagoner, J.C., eds. Sea Level Changes: An Integrated Approach: SEPM Special Publication 42, p. 39-45.

Van Wagoner, J.C., Mitchum, R.M., Campion, K.M., Rahamian, V.D., 1990, Siliciclastic Sequence Stratigraphy in Well Logs, Cores and Outcrops: Concepts for High-Resolution Correlation of Time and Facies: AAPG Methods in Exploration Series, no. 7, 55p.

Zarra, L., 1989, Sequence Stratigraphy and Foraminiferal Biostratigraphy for Selected Wells in the Albemarle Embayment, North Carolina: North Carolina Geological Survey Open File Report 89-5.

Zullo, V.A., and Harris, W.B, 1987, Sequence stratigraphy, biostratigraphy and correlation of Eocene through Miocene strata in North Carolina, in Ross, C.A., and Haman, D., eds. Timing and depositional history of eustatic sequences: Constraints on seismic stratigraphy: Cushman Foundation for Foraminiferal Research Special Publication 24, p. 197-214.

APPENDIX

Appendix 1. Results of insoluble residue analysis. KBC = Kure Beach core, HPC = Hilton Park core, BRC = Black Rock Landing core.

Sample #	Depth (ft.)	% Carbonate	% Sand	% Mud	Sample #	Depth	% Carbonate	% Sand	% Mud
KBC-01	130.1	21.41	29.07	49.52	KBC-32	268.6	46.44	17.26	36.30
KBC-02	135.6	21.47	23.18	55.35	KBC-33	273.6	46.53	22.09	31.38
KBC-03	140.1	5.94	77.83	16.24	KBC-34	278.9	47.00	13.93	39.07
KBC-04	145.2	7.28	80.65	12.08	KBC-35	283.7	48.99	17.40	33.61
KBC-05	147.9	8.09	81.78	10.13	KBC-36	293.5	52.56	21.33	26.10
KBC-06	150.8	86.40	8.86	4.74	KBC-37	296.1	39.94	23.29	36.77
KBC-07	155.1	78.21	18.01	3.78	KBC-38	300	26.32	41.08	32.59
KBC-08	160.6	63.53	32.54	3.93	KBC-39	305.5	30.86	39.63	29.51
KBC-09	162.5	56.72	34.98	8.29	KBC-40	306.7	31.78	35.56	32.66
KBC-10	165.5	68.97	26.33	4.70	KBC-41	310.3	32.79	34.31	32.91
KBC-11	168.65	44.40	53.62	1.98	KBC-42	314.3	32.84	36.13	31.02
KBC-12	171.12	52.57	43.92	3.50	KBC-43	315.7	42.62	24.35	33.04
KBC-13	175.1	72.65	25.36	1.99	KBC-44	323.4	41.35	38.55	20.10
KBC-14	180.3	68.13	28.05	3.81	KBC-45	325.3	39.28	43.98	16.74
KBC-15	185.3	41.08	53.21	5.71	KBC-46	333.4	42.58	44.68	12.74
KBC-16	190.5	49.55	46.04	4.42	KBC-47	342.5	27.51	60.63	11.86
KBC-17	191.9	43.32	52.83	3.84	KBC-48	344.9	thin sectioned		
KBC-18	200.3	52.59	44.95	2.45	KBC-49	350.8	24.11	66.03	9.87
KBC-19	204.92	46.10	49.95	3.96	KBC-50	354.8	62.39	26.46	11.15
KBC-20	210.12	51.69	46.81	1.50	KBC-51	360.6	38.44	42.81	18.75
KBC-21	215.1	66.64	27.25	6.11	KBC-52	364.7	39.36	42.58	18.07
KBC-22	217.85	35.03	60.66	4.31	KBC-53	366.4	42.41	40.62	16.97
KBC-23	224.9	32.35	64.68	2.98	KBC-54	371.1	37.68	46.87	15.45
KBC-24	231.1	74.24	21.05	4.71	KBC-55	373.1	thin sectioned		
KBC-25	240.25	47.30	41.20	11.50	KBC-56	374.3	65.76	11.15	23.10
KBC-26	251.15	46.18	37.39	16.42	KBC-57	381.1	60.80	13.22	25.99
KBC-27	253.35	47.90	34.98	17.13	KBC-58	383.7	64.18	15.10	20.72
KBC-28	257.35	49.80	28.83	21.37	KBC-59	386.9	69.78	8.81	21.40
KBC-29	258.4	66.42	13.86	19.73	KBC-60	390.7	65.52	7.47	27.01
KBC-30	260.6	53.21	17.87	28.92	KBC-61	395.2	thin sectioned		
KBC-31	265.8	44.27	23.26	32.48	KBC-62	400.7	29.31	48.95	21.74

Appendix 1. Results of insoluble residue analysis. KBC = Kure Beach core, HPC = Hilton Park core, BRC = Black Rock Landing core, continued.

Sample #	Depth	% Carbonate	% Sand	% Mud
KBC-63	403.1	35.08	40.86	24.06
KBC-64	407.7	20.48	58.53	20.99
KBC-65	412.4	27.97	54.83	17.20
KBC-66	417.9	23.72	69.29	6.99
KBC-67	420.1	22.96	69.15	7.89
KBC-68	430.1	33.15	49.47	17.38
KBC-69	440.1	30.42	44.01	25.57
KBC-70	441.1	22.55	67.88	9.57
KBC-71	442.1	21.67	61.21	17.13
KBC-72	443.8	22.80	44.19	33.01
KBC-73	446.9	17.03	60.11	22.86
KBC-74	450	17.16	59.14	23.70
KBC-75	450.3	23.03	38.62	38.35
KBC-76	452.7	20.93	56.33	22.74
KBC-77	458.3	27.54	36.41	36.05
KBC-78	461.2	25.52	40.18	34.30
KBC-79	463.9	36.06	33.02	30.92
KBC-80	466.4	34.82	34.61	30.57
HPC-01	29.1	33.37	44.07	22.57
HPC-02	30.9	55.23	31.10	13.68
HPC-03	34.9	30.28	44.33	25.40
HPC-04	38.4	15.67	58.33	26.00
HPC-05	41.6	29.81	36.93	33.26
HPC-06	44.7	18.77	51.95	29.29
HPC-07	47.1	63.61	31.20	5.19
HPC-08	51.9	33.55	60.27	6.19
HPC-09	57.2	67.13	30.00	2.86
HPC-10	61.4	58.07	37.93	4.01
BRC-01	29.1	23.61	22.85	53.54
BRC-02	31.2	17.27	27.84	54.89
BRC-03	33.2	16.84	26.45	56.71
BRC-04	36.7	10.84	36.01	53.15
BRC-05	41.7	10.45	52.27	37.28
BRC-06	43.4	6.27	67.63	26.11
BRC-07	47.1	36.43	43.12	20.45
BRC-08	49.9	5.18	72.79	22.03
BRC-09	53.9	19.89	61.47	18.64

Appendix 2. Folk and Ward (1957) grain size statistics. KBC = Kure Beach core, HPC = Hilton Park core, BRC = Black Rock Landing core.

Sample #	Plot depth	Mean	Median	Std. Dev.	Skewness	Kurtosis
KBC-01	130.1	0.07	-1.46	2.13	0.78	1.58
KBC-02	135.6	2.59	2.96	0.87	0.63	1.09
KBC-03	140.1	2.87	2.39	0.53	0.46	1.37
KBC-04	145.2	2.67	2.14	0.53	0.12	4.59
KBC-05	147.9	2.53	2.06	0.63	-0.78	5.44
KBC-06	150.8	2.39	1.93	1.45	0.16	0.49
KBC-07	155.1	1.40	0.98	0.69	0.26	2.10
KBC-08	160.6	1.64	1.13	0.63	-0.07	3.03
KBC-09	162.5	1.73	1.19	0.76	-0.17	2.90
KBC-10	165.5	1.36	0.89	0.75	0.17	0.77
KBC-11	168.65	1.49	1.00	0.64	-0.04	2.70
KBC-12	171.12	1.43	0.97	0.59	0.05	3.17
KBC-13	175.1	1.11	0.65	0.97	-0.09	1.81
KBC-14	180.3	1.44	0.96	0.81	0.13	1.52
KBC-15	185.3	2.18	1.76	0.61	-0.41	2.68
KBC-16	190.5	1.84	1.29	0.62	0.33	2.44
KBC-17	191.9	1.96	1.52	0.70	-0.36	2.96
KBC-18	200.3	1.77	1.27	0.62	0.02	2.04
KBC-19	204.92	1.99	1.48	0.60	0.01	1.98
KBC-20	210.12	1.78	1.25	0.66	0.01	2.29
KBC-21	215.1	2.71	2.19	0.55	0.73	2.17
KBC-22	217.85	2.40	1.96	0.44	-0.15	4.89
KBC-23	224.9	2.20	1.78	0.53	-0.36	2.02
KBC-24	231.1	2.63	2.10	0.59	0.35	2.51
KBC-25	240.25	2.53	2.02	0.41	0.27	6.02
KBC-26	251.15	2.96	2.55	0.55	0.26	0.86
KBC-27	253.35	3.04	2.62	0.55	-0.12	0.84
KBC-28	257.35	3.05	2.69	0.56	-0.06	0.81
KBC-29	258.4	3.09	2.67	0.63	-0.27	0.69
KBC-30	260.6	3.09	2.69	0.64	-0.54	1.40
KBC-31	265.8	3.09	2.66	0.61	-0.23	1.32
KBC-32	268.6	3.07	2.77	0.65	-0.37	1.39
KBC-33	273.6	3.15	2.88	0.50	-0.21	1.05
KBC-34	278.9	3.05	2.84	0.65	0.07	0.81
KBC-35	283.7	3.23	2.91	0.50	-0.95	2.78
KBC-36	293.5	3.18	2.89	0.48	-0.39	1.22
KBC-37	296.1	3.18	2.87	0.50	-0.67	2.03
KBC-38	300	2.81	2.44	0.64	0.13	1.78
KBC-39	305.5	2.87	2.44	0.64	-0.17	1.85
KBC-40	306.7	2.66	2.47	1.34	-2.07	6.83
KBC-41	310.3	2.81	2.49	0.72	-0.88	7.17
KBC-42	314.3	2.74	2.49	0.77	-0.19	2.01
KBC-43	315.7	2.80	2.53	0.75	-0.10	1.53
KBC-44	323.4	1.75	1.27	0.86	0.17	2.10
KBC-45	325.3	1.69	1.19	0.80	-0.11	2.58

Appendix 2. Folk and Ward (1957) grain size statistics. KBC = Kure Beach core, HPC = Hilton Park core, BRC = Black Rock Landing core, continued.

Sample #	Plot depth	Mean	Median	Std. Dev.	Skewness	Kurtosis
KBC-46	333.4	2.23	1.82	0.63	-0.46	3.03
KBC-47	342.5	2.24	1.83	0.54	-0.49	2.99
KBC-48	344.9	Thin sectioned				
KBC-49	350.8	2.36	1.94	0.41	-0.75	4.82
KBC-50	354.8	2.37	1.96	0.52	0.08	3.50
KBC-51	360.6	2.39	1.95	0.51	-0.22	3.91
KBC-52	364.7	2.40	1.95	0.60	-0.47	4.00
KBC-53	366.4	2.38	1.93	0.50	-0.61	4.43
KBC-54	371.1	2.51	2.02	0.42	0.47	6.44
KBC-55	373.1	Thin sectioned				
KBC-56	374.3	2.67	2.39	0.89	0.57	0.95
KBC-57	381.1	2.89	2.60	0.72	0.42	0.73
KBC-58	383.7	3.12	2.81	0.62	-0.32	1.02
KBC-59	386.9	3.00	2.66	1.11	-0.16	0.49
KBC-60	390.7	2.91	2.74	1.57	0.25	1.28
KBC-61	395	Thin sectioned				
KBC-62	400.7	3.17	2.86	0.52	-0.17	3.72
KBC-63	403.1	2.49	2.26	1.10	-0.39	1.59
KBC-64	407.7	1.75	1.12	1.11	0.41	2.08
KBC-65	412.4	1.49	0.98	0.78	0.44	3.60
KBC-66	417.9	1.56	1.04	0.74	0.29	2.89
KBC-67	420.1	1.70	1.17	0.76	0.23	2.56
KBC-68	430.1	1.87	1.33	0.79	-0.01	2.84
KBC-69	440.1	1.80	1.27	0.80	-0.07	3.10
KBC-70	441.1	2.31	1.89	0.47	-0.49	3.34
KBC-71	442.1	1.77	1.23	0.74	0.17	3.08
KBC-72	443.8	1.83	1.27	0.75	0.40	2.64
KBC-73	446.9	1.64	1.13	0.77	-0.37	4.70
KBC-74	450	1.73	1.19	0.72	0.24	2.63
KBC-75	450.3	1.67	1.13	0.82	0.44	2.66
KBC-76	452.7	1.71	1.17	0.77	0.25	2.55
KBC-77	458.3	1.75	1.17	0.89	0.44	2.37
KBC-78	461.2	1.91	1.32	0.97	0.32	1.98
KBC-79	463.9	2.17	1.54	1.01	-0.04	1.67
KBC-80	466.4	2.35	1.87	1.03	-0.38	1.87

Appendix 2. Folk and Ward (1957) grain size statistics. KBC = Kure Beach core, HPC = Hilton Park core, BRC = Black Rock Landing core, continued.

Sample #	Plot depth	Mean	Median	Std. Dev.	Skewness	Kurtosis
HPC-01	29.1	2.96	2.51	0.58	-0.08	1.45
HPC-03	34.9	2.93	2.69	0.81	-0.12	2.98
HPC-04	38.4	2.48	2.02	0.63	-0.43	4.27
HPC-05	41.6	2.69	2.22	0.65	0.14	2.04
HPC-06	44.7	2.62	2.10	0.57	0.26	2.87
HPC-07	47.1	2.37	1.96	0.49	0.09	3.85
HPC-08	51.9	2.49	2.00	0.37	0.10	7.24
HPC-09	57.2	2.25	1.84	0.68	-0.56	3.01
HPC-10	61.4	2.39	1.96	0.49	-0.71	5.64
BRC-01	29.1	3.12	2.81	0.56	-0.46	1.59
BRC-02	31.2	3.19	2.91	0.64	-0.43	2.97
BRC-03	33.2	3.36	2.94	0.35	-0.67	3.07
BRC-04	36.7	3.30	2.92	0.53	-0.37	3.55
BRC-05	41.7	1.71	1.16	1.21	-0.32	2.85
BRC-06	43.4	1.80	1.28	0.84	0.05	2.50
BRC-07	47.1	1.78	1.23	0.90	0.23	2.12
BRC-08	49.9	1.73	1.23	0.85	-0.12	2.61
BRC-09	29.1	1.90	1.45	0.82	-0.19	2.51

Appendix 3. Relative abundance of components. KBC = Kure Beach core, HPC = Hilton Park core, BRC = Black Rock Landing core. D = Dominant (>75%), VA = Very Abundant (51-75%), A = Abundant (26-50%), C = Common (15-25%), R = Rare (1-15%), T = Trace (<1%), - = Not observed.

Sample Number	Depth (ft.)	Quartz	Glauconite	Phosphate	Mica	Heavy Minerals	Fe-Ox.	Silicified Shells	Lithoclasts
KBC-01	130.1	A	T	T	R	T	T	-	-
KBC-02	135.6	D	R	R	R	T	T	-	-
KBC-03	140.1	D	R	T	R	T	T	-	-
KBC-04	145.2	D	R	T	R	T	T	T	-
KBC-05	147.9	VA	C	T	R	T	T	T	-
KBC-06	150.8	D	R	R	R	T	T	R	-
KBC-07	155.1	D	T	T	T	T	T	-	-
KBC-08	160.6	D	T	R	T	T	T	R	-
KBC-09	162.5	D	T	T	T	T	T	R	-
KBC-10	165.4	D	T	T	T	T	T	T	-
KBC-11	168.7	D	T	T	T	T	T	-	-
KBC-12	171.1	D	T	T	T	T	T	-	-
KBC-13	175.1	D	T	T	T	T	T	-	-
KBC-14	180.3	D	T	T	T	T	T	-	-
KBC-15	185.3	D	T	R	T	T	T	-	-
KBC-16	191	D	T	T	T	T	T	-	-
KBC-17	191.9	D	T	T	T	T	T	-	-
KBC-18	200.3	D	T	T	T	T	T	-	-
KBC-19	204.9	D	T	T	T	T	T	-	-
KBC-20	210.1	D	T	T	T	T	T	-	-
KBC-21	215.1	D	T	T	R	T	R	-	-
KBC-22	217.9	D	T	R	R	T	R	-	-
KBC-23	224.9	D	T	R	R	T	T	-	-
KBC-24	231.1	D	R	R	R	T	T	-	-

Appendix 3. Relative abundance of components. KBC = Kure Beach core, HPC = Hilton Park core, BRC = Black Rock Landing core. D = Dominant (>75%), VA = Very Abundant (51-75%), A = Abundant (26-50%), C = Common (15-25%), R = Rare (1-15%), T = Trace (<1%), - = Not observed, continued.

Sample Number	Depth (ft.)	Quartz	Glauconite	Phosphate	Mica	Heavy Minerals	Fe-Ox.	Silicified Shells	Lithoclasts
KBC-25	240.2	D	R	R	R	T	T	-	-
KBC-26	251.1	VA	R	R	R	T	T	-	-
KBC-27	253.4	VA	R	R	R	T	T	-	-
KBC-28	257.3	VA	R	R	R	T	T	-	-
KBC-29	258.4	VA	R	R	R	T	T	-	-
KBC-30	260.6	VA	R	R	R	T	T	-	-
KBC-31	265.8	D	R	R	R	T	T	-	-
KBC-32	268.5	VA	R	R	R	T	T	-	-
KBC-33	273.6	VA	R	R	R	T	T	-	R
KBC-34	283.8	VA	R	R	R	T	T	-	-
KBC-35	278.9	VA	R	R	R	T	T	-	-
KBC-36	293.4	VA	R	R	R	T	T	-	-
KBC-37	296.2	VA	R	R	R	T	T	-	-
KBC-38	301	VA	R	R	R	T	T	-	-
KBC-39	305.5	VA	R	R	R	T	T	-	-
KBC-40	306.7	VA	R	R	R	T	T	-	-
KBC-41	310.3	VA	R	R	R	T	T	-	-
KBC-42	314.2	VA	C	R	R	T	T	-	-
KBC-43	315.6	VA	C	R	R	T	T	-	-
KBC-44	323.4	D	R	R	T	T	R	-	-
KBC-45	325.3	D	R	R	T	T	T	-	-
KBC-46	333.4	D	R	R	T	T	T	-	-
KBC-47	342.5	D	R	T	R	T	T	-	-
KBC-48	344.7								
KBC-49	350.8	D	R	T	R	T	T	-	-

Appendix 3. Relative abundance of components. KBC = Kure Beach core, HPC = Hilton Park core, BRC = Black Rock Landing core. D = Dominant (>75%), VA = Very Abundant (51-75%), A = Abundant (26-50%), C = Common (15-25%), R = Rare (1-15%), T = Trace (<1%), - = Not observed, continued.

Sample Number	Depth (ft.)	Quartz	Glauconite	Phosphate	Mica	Heavy Minerals	Fe-Ox.	Silicified Shells	Lithoclasts
KBC-50	354.8	D	R	T	R	T	T	-	-
KBC-51	360.6	D	R	R	R	T	T	-	-
KBC-52	364.7	D	R	R	R	T	T	-	-
KBC-53	366.4	D	R	R	R	T	T	-	-
KBC-54	371.1	D	R	R	R	T	T	-	-
KBC-55	373.1								
KBC-56	374.3	VA	R	T	R	T	T	-	T
KBC-57	381.1	VA	R	R	R	T	T	-	-
KBC-58	383.7	VA	R	R	R	T	T	-	-
KBC-59	386.9	D	R	R	R	T	T	-	-
KBC-60	390.7	D	R	R	R	T	T	-	-
KBC-61	395.2								
KBC-62	400.7	D	R	T	R	T	T	-	-
KBC-63	403.1	D	R	T	R	T	T	-	-
KBC-64	407.7	VA	A	T	T	T	T	-	-
KBC-65	412.4	D	C	T	T	T	T	-	-
KBC-66	417.9	VA	A	T	T	T	T	-	-
KBC-67	420.1	VA	A	T	T	T	T	-	-
KBC-68	430.1	C	VA	T	T	T	T	-	-
KBC-69	440.1	C	D	T	T	T	T	-	-
KBC-70	441.3	D	R	T	T	T	T	-	-
KBC-71	442.1	C	VA	T	T	T	T	-	-
KBC-72	443.8	A	VA	T	T	T	T	-	-
KBC-73	446.8	D	R	T	T	T	T	-	-

Appendix 3. Relative abundance of components. KBC = Kure Beach core, HPC = Hilton Park core, BRC = Black Rock Landing core. D = Dominant (>75%), VA = Very Abundant (51-75%), A = Abundant (26-50%), C = Common (15-25%), R = Rare (1-15%), T = Trace (<1%), - = Not observed, continued.

Sample Number	Depth (ft.)	Quartz	Glauconite	Phosphate	Mica	Heavy	Fe-Ox.	Silicified Shells	Lithoclasts
KBC-75	450.3	D	R	T	T	T	T	-	T
KBC-76	452.7	D	R	T	T	T	T	-	T
KBC-77	458.3	VA	C	T	T	T	T	-	-
KBC-78	44.3	VA	C	T	T	T	T	-	T
KBC-79	461.3	VA	C	T	T	T	T	-	-
KBC-80	466.4	VA	A	T	T	T	T	-	-
HPC-01	29.1	D	R	R	R	T	T	-	-
HPC-02	30.9	D	R	R	R	T	T	T	-
HPC-03	34.9	D	R	R	R	T	T	T	-
HPC-04	38.4	D	R	R	R	T	R	-	-
HPC-05	41.6	D	T	R	R	T	T	-	-
HPC-06	44.7	D	R	R	R	T	T	-	-
HPC-07	47.1	D	R	T	R	T	T	-	-
HPC-08	51.9	D	R	R	R	T	T	-	-
HPC-09	57.2	D	R	R	R	T	T	-	-
BRC-03	33.2	VA	R	R	R	T	T	-	-
BRC-04	36.7	VA	R	R	R	T	T	-	-
BRC-05	41.7	D	R	T	T	T	T	-	-
BRC-06	43.4	D	R	R	R	T	T	-	-
BRC-07	47.1	D	T	T	T	T	T	-	-
BRC-08	49.9	D	R	R	R	T	R	-	R
BRC-09	53.9	D	R	T	T	T	T	-	-

Appendix 4. Results of Kure Beach thin section point counts (200 points). Values in columns are given in volume percent.

Sample Number	Depth (ft.)	Void Space	Matrix	Other Allochems	Benthic Foraminifera	Planktonic Foraminifera	Unknown Mollusk Fragments	Echinoid Fragments	Ostracodes	Crinoid Columnals	Mollusk Fragments	Bryozoans
KBC-06	150.8	12	43	5.5	2	-	5	-	-	-	-	-
KBC-07	155.1	19	26.5	17.5	5.5	-	13	1	1.5	-	-	-
KBC-08	160.6	15.5	32	10.5	4	-	10	0.5	2	-	1.5	1
KBC-13	175.1	24	13	15	2	-	10	1.5	4	-	-	-
KBC-14	180.3	10	24.5	12.5	4	-	3.5	-	3	-	-	-
KBC-20	210.1	4	19	7.5	10.5	1.5	-	1	1	-	-	-
KBC-23	224.9	1	26.5	12.5	17	7.5	4	1	3	-	-	-
KBC-24	231.1	4	22.5	12.5	12	3	2.5	3	5	-	-	-
KBC-25	240.2	12	28	12	6	-	11	3.5	3.5	-	-	-
KBC-48	344.9	10.5	17	4	4.5	1.5	7.5	2	-	-	-	-
KBC-50	354.8	4.5	22	12	10.5	3	5.5	4	3.5	-	-	-
KBC-55	373.1	0.5	22	20.5	12	3.5	6	4	2.5	1	0.5	-
KBC-61	395.2	8.5	22.5	11	10	4.5	9.5	6.5	1	2.5	-	-

Appendix 5. Relative abundance of allochems in selected Kure Beach core samples examined by binocular microscope. C = Common (16-25%), R = Rare (1-15%), T = Trace (<1%), - = Not observed.

Sample	Depth (ft.)	Benthic Foraminifera	Mollusk Fragments	Echinoid Fragments	Crinoid nnals
KBC-29	254.8	C	T	T	-
KBC-36	293.4	R	R	R	-
KBC-43	315.6	R	T	T	R
KBC-58	383.7	R	C	T	R
KBC-60	390.7	R	R	-	R

Appendix 6. Locations of Cretaceous exposures downstream of Lock and Dam #1, Cape Fear River, N.C

Exposure	Latitude (° N)	Longitude (° W)
Kings Bluff	34° 24' 05"	78° 17' 20"
Black Rock Landing	34° 23' 47"	78° 16' 06"
Mitchell Landing	34° 21' 28"	78° 12' 38"
Sykes Landing	34° 21' 16"	78° 10' 17"
Greenbank Landing	34° 21' 31"	78° 09' 30"
Wanets Landing	34° 21' 53"	78° 08' 25"
Strawberry Hill Landing	34° 20' 15"	78° 03' 52"

BIOGRAPHICAL SKETCH

Jessica Ann Pierson was born on August 14, 1979 in Clarksburg, West Virginia. In May 2001, she received a Bachelor of Science Degree in geology from West Virginia University. That fall, she entered the graduate program in Earth Sciences at the University of North Carolina at Wilmington under the direction of Dr. William Burleigh Harris. While attending the University of North Carolina at Wilmington, she served as a teaching assistant for *Introduction to Physical Geology* for the Department of Earth Sciences. She also served as a National Science Foundation GK-12 Teaching Fellow in Wilmington middle schools. She currently resides in Raleigh, N.C. and is employed with the North Carolina Geological Survey at its Coastal Plains Office.